TOXICOLOGICAL SCIENCES **98(2)**, 348–365 (2007)
doi:10.1093/toxsci/kfm119
Advance Access publication May 15, 2007

An Age-Dependent Physiologically Based Pharmacokinetic/ Pharmacodynamic Model for the Organophosphorus Insecticide Chlorpyrifos in the Preweanling Rat

Charles Timchalk,[1] Ahmed A. Kousba,[2] and Torka S. Poet

Battelle Pacific Northwest Division, Center for Biological Monitoring and Modeling, Richland, Washington 99352

Received January 5, 2007; accepted May 8, 2007

Juvenile rats are more susceptible than adults to the acute toxicity of organophosphorus insecticides like chlorpyrifos (CPF). Age- and dose-dependent differences in metabolism may be responsible. Of importance are CYP450 activation and detoxification of CPF to chlorpyrifos-oxon (CPF-oxon) and trichloropyridinol (TCP), as well as B-esterase (B-est) and PON-1 (A-esterase) detoxification of CPF-oxon to TCP. In the current study, a physiologically based pharmacokinetic/pharmacodynamic (PBPK/PD) model incorporating age-dependent changes in CYP450, PON-1, and tissue B-est levels for rats was developed. In this model, age was used as a dependent function to estimate body weight which was then used to allometrically scale both metabolism and tissue cholinesterase (ChE) levels. In addition, age-dependent changes in brain, liver, and fat volumes and brain blood flow were obtained from the literature and used in the simulations. Model simulations suggest that preweanling rats are particularly sensitive to CPF toxicity, with levels of CPF-oxon in blood and brain disproportionately increasing, relative to the response in adult rats. This age-dependent nonlinear increase in CPF-oxon concentration may potentially result from both the depletion of nontarget B-est and a lower PON-1 metabolic capacity in younger animals. The PBPK/PD model behaves consistently with the general understanding of CPF toxicity, pharmacokinetics, and tissue ChE inhibition in neonatal and adult rats. Hence, this model represents an important starting point for developing a computational model to assess the neurotoxic potential of environmentally relevant organophosphate exposures in infants and children.

Key Words: **chlorpyrifos; PBPK/PD; preweanling rat; age-dependent sensitivity.**

There is currently a significant concern and focus over the potential increased sensitivity of infants and children to the toxic effects of chemicals. The importance of this issue is highlighted by the National Research Council's report *on Pesticides in the Diets of Infants and Children* (National Academy of Sciences, 1993) and the establishment of the *Food Quality Protection Act* (FQPA, 1996). Children are not small adults, but rather a unique subpopulation that may have altered vulnerability to chemical insult. Age-dependent changes in a child's physiology (i.e., body size, blood flow, organ functions) and metabolic capacity (i.e., phase I and II metabolism) may significantly impact their response to a chemical insult, resulting in either beneficial or detrimental effects (Alcorn and McNamara, 2002; Ginsberg *et al.*, 2004; Johnson, 2003; Makri *et al.*, 2004; Miller *et al.*, 1997). Clear age-dependent variability in the capacity to detoxify environmental chemicals has been established in both animals and humans. However, the current risk assessment paradigms may not adequately consider the implications of these differences on the risk to infants and children.

Numerous studies have demonstrated that juvenile animals are more susceptible to the acute effects of organophosphorus (OP) insecticides than adults (Benke and Murphy, 1975; Brodeur and DuBois, 1963; Gaines and Linder, 1986; Harbison, 1975; Moser and Padilla, 1998; Pope and Liu, 1997; Pope *et al.*, 1991). The primary toxicological effect of OP insecticides is associated with the inhibition of acetylcholinesterase (AChE) in both central and peripheral nerve tissues (Murphy, 1986; Sultatos, 1994). The greater neonatal sensitivity has primarily been attributed to the lack of complete metabolic competence during development (Benke and Murphy, 1975). In this regard age-dependent sensitivity may be associated with maturational differences in CYP450 activation/detoxification, detoxification by PON-1 and B-esterase [B-est; AChE, butyrylcholinesterase (BuChE) and carboxylesterase (CaE)] enzyme activity (Atterberry *et al.*, 1997; Li *et al.*, 1997; Mortensen *et al.*, 1996, 1998). These findings in animals are in agreement with observations in which newborn and young humans have lower metabolic capacity for CYP450 and PON-1 activity compared to adults (Augustinsson and Barr, 1963; Johnson, 2003; Mueller *et al.*, 1983).

The application of physiologically based pharmacokinetic/ pharmacodynamic (PBPK/PD) modeling offers a unique opportunity to integrate age-dependent changes in metabolic activation and detoxification pathways into a comprehensive model that is

[1] To whom correspondence should be addressed at Battelle Pacific Northwest Division, Center for Biological Monitoring and Modeling, 902 Battelle Boulevard, Richland, WA 99352. Fax: (509) 376-9064. E-mail: charles.timchalk@pnl.gov.

[2] Current address: TargeGen Inc., 9380 Judiccial Dr., San Diego, CA 92121.

capable of quantifying dosimetry and response across all ages (for review see Corley *et al.*, 2003). In this context, PBPK models are being extended to the modeling of chemical exposure in developing/juvenile animals and in children (Byczkowski *et al.*, 1994; Clewell *et al.*, 2002, 2003, 2004; Fisher *et al.*, 1990; Price *et al.*, 2003; Sundberg *et al.*, 1998).

A PBPK/PD model (see Fig. 1A) has been previously developed for the phosphorothionate insecticide chlorpyrifos (CPF) ([*O*,*O*′-diethyl (*O*-3,5,6-trichloro-2-pyridyl) phosphorothionate]) (Timchalk *et al.*, 2002). CPF does not directly inhibit AChE, but must first undergo CYP450 mediated oxidative desulfation, to form chlorpyrifos-oxon (CPF-oxon) as is illustrated in Figure 1B (Chambers and Chambers, 1989; Murphy, 1986; Sultatos, 1994). A balance between the extent of metabolic activation and detoxification determines individual susceptibility to the toxicity of this compound and is most likely associated with individual and age-dependent sensitivity (Ma and Chambers, 1994). The working hypothesis is that a decrement in CYP450 and/or esterase (PON-1 and B-est)–mediated detoxification alters the balance between activation and detoxification and correlates with increased sensitivity of young animals and the significant variability in human sensitivity to OP insecticides. To address this issue, the previously published CPF PBPK/PD model (Timchalk *et al.*, 2002) was modified by incorporating age-dependent scaling to adjust physiology, organ volumes, and blood flows, metabolism rates, B-est tissue levels, and bimolecular inhibition rates for CPF-oxon and AChE as a function of age. The model was then used to predict tissue dosimetry, and pharmacodynamic (PD) response (i.e., esterase inhibition) in preweanling and adult rats exposed to CPF. The ultimate goal is to apply this model to evaluate the risk associated with environmental exposure of infants and children to OP insecticides.

MATERIALS AND METHODS

Model structure. A diagram of the PBPK/PD model structure is illustrated in Figure 1A. The CPF model was developed to describe the time-course of CPF, CPF-oxon, and TCP, as well as the inhibition of target esterases by the oxon in adult rats and humans, and was originally based on the model developed for diisopropylfluorophosphate by Gearhart *et al.* (1990). New research has made it possible to update a number of key model parameters including those associated with ChE inhibition, metabolism, and tissue partition for CPF and CPF-oxon (Kousba *et al.*, 2004, 2007; Lowe *et al.*, 2006; Timchalk *et al.*, 2002). Briefly, in the model CYP450 mediated activation of CPF to CPF-oxon and detoxification to TCP occurs only in the liver and is described as a Michaelis–Menten process. PON-1 mediated metabolism of CPF-oxon occurs in the liver and blood and is likewise described as a Michaelis–Menten process. Interaction of CPF-oxon with the B-esterases (B-est) AChE, BuChE, and CaE is modeled as a second-order process occurring in the liver, blood, diaphragm, and brain. The B-est enzyme levels (μmol) in blood (plasma and red blood cells[RBC]), brain, liver, and diaphragm were calculated based on the enzyme turnover rates and enzyme activities reported by Maxwell *et al.* (1987), and these were based on a balance between basal degradation and enzyme synthesis. In the model scaling equations were developed to address age-dependent changes in CYP450, PON-1, and B-est activity in the rat.

Model parameters. To develop the model, physiological constants, partition coefficients, and biochemical constants were obtained from the literature, through experimentation, or via optimization of model output using computer simulation. The PBPK/PD model code for simultaneous solution of both algebraic and differential equations was originally developed in SIMUSOLV (The Dow Chemical Co., Midland, MI), and adapted to acslXtreme (Aegis Technology, Huntsville, AL) for sensitivity analysis. The model parameter estimates that were used to describe the adult CPF pharmacokinetic and PD responses are presented in Tables 1 and 3; for a more detailed description of the sources and rational for parameter estimates see Timchalk *et al.* (2002). In addition, the model code, parameter estimates, and data files used as part of this PBPK/PD model have been posted with *Toxicological Sciences* as Supplemental Data (for model code, experimental data, and model parameters see supplemental data files 7, 8, and 9 for additional details).

Parameter scaling. To simulate the kinetics of CPF dosimetry and ChE inhibition in neonatal rats, the PBPK/PD model was modified to scale metabolism and ChE activity as a function of age, allometric scaling equations, and parameter estimates are presented in Tables 2 and 4. A polynomial equation was fit to the age-dependent body weight data for Sprague–Dawley rats (up to 75 days of age) using published values from male neonates (Carr *et al.*, 2001), and from the historical body weight ranges obtained from the animal supplier (Charles River Laboratory, Raleigh, NC). A similar scaling approach was used to fit age-dependent changes in liver and brain volumes using compiled data (Gentry *et al.*, 2004). As illustrated in Figure 2, the polynomial equations accurately reflected body weight, liver, and brain volume as a function of age in the Sprague–Dawley rat, up to ~60–75 days of age. Body weights were then used to allometrically scale both metabolism rates and tissue esterase levels, whereas liver and brain volume changes were calculated and used directly in the model (see supplemental data files 1, 2, and 3 for additional details).

To allometrically scale CPF and CPF-oxon metabolism in the preweanling rat, *in vitro* data on age-dependent CYP450 and PON-1 metabolism were utilized (Atterberry *et al.*, 1997). In the adult rat and human PBPK/PD model (Timchalk *et al.*, 2002) *in vitro* metabolic rates were scaled across species as a function of body weight utilizing a standard allometric approach ($Bwt^{0.74}$), which is consistent with the commonly used methods for adults (e.g., Krishnan and Andersen, 1994). However, applying this scaling factor to preweanling rats resulted in a substantial overestimate of the *in vivo* metabolism, based on model simulations (data not shown). As previously reported by Atterberry *et al.* (1997) the age-dependent increase in CYP450 metabolic activity paralleled the increase in the amount of hepatic CYP450 enzyme. Hence, the age-dependent preweanling CYP450 as well as PON-1 activity was based upon the experimentally measured *in vivo* results (see Atterberry *et al.*, 1997), utilizing a modified allometric scaling equation, and the overall fit to the experimental results are presented in Figure 3A. The modification to the allometric equation is illustrated in Equation 1 and the individual equations ($Vmax_{(1–4)}$) with their specific parameter estimates are presented in Table 2. As is illustrated in Equation 1, the age-dependent Vmax for CYP450 or PON-1 activity was determined for each age by adjusting the VmaxC by a scaling factor (VmSC) and the exponent for the body weight adjustment (Bwt^n). Based on this approach allometric scaling was utilized to determine $Vmax_{(1–4)}$ for both the CYP450 and PON-1 metabolism and was used to scale metabolism in preweanling through adult rats (see supplemental data file 6 for more details).

$$\mathrm{Vmax} = (\mathrm{VmSC} \times \mathrm{VmaxC}) \times \mathrm{Bwt}^n \quad (1)$$

B-esterase (B-est) scaling. The amount of tissue ChE (AChE and BuChE) and CaE were also allometrically scaled based upon age-dependent changes in published preweanling tissue enzyme levels (Atterberry *et al.*, 1997; Carr *et al.*, 2001; Mortensen *et al.*, 1998, 1998; Tang *et al.*, 1999), and the enzyme activity ($B\text{-}estC_{(1–12)}$; μmol/h/kg) for each tissue was calculated (see Table 4) based on the enzyme turnover rates and activities reported by Maxwell *et al.* (1987). For plasma AChE the enzyme activity (Maxwell *et al.*, 1987) was increased from 523 to 5230 μmol/h/kg in order to reasonably simulate the time-course of ChE inhibition (see Table 4) at all ages (see supplemental data files 4 and 5 for additional details). For the liver and diaphragm compartments where age-dependent enzyme activity was not available the default scaling was arbitrarily based on the plasma. The basal levels of RBC AChE were calculated

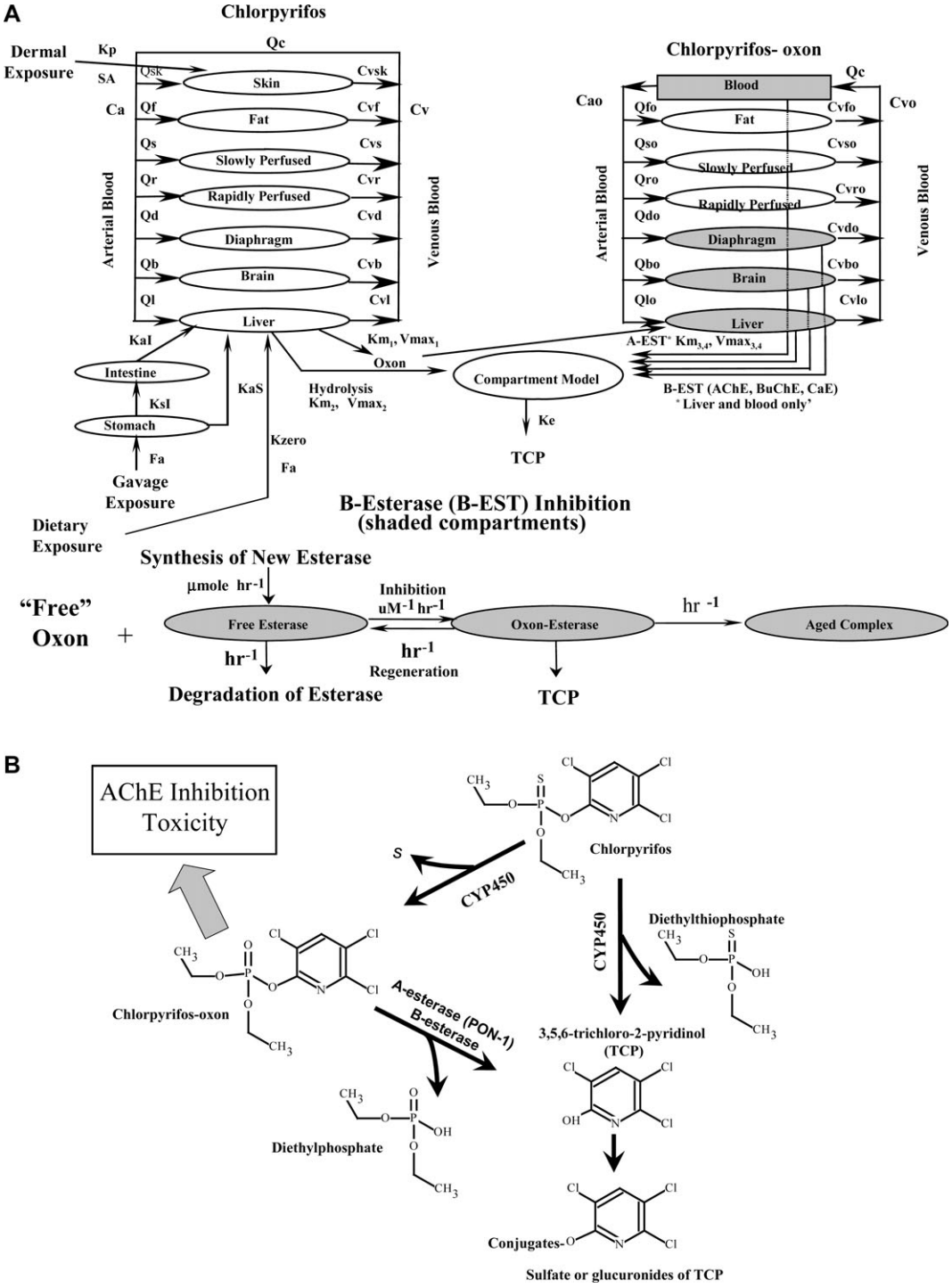

FIG. 1. (A) PBPK/PD model used to describe the disposition of the parent insecticide CPF, its oxon metabolite (CPF-oxon), TCP, and B-est inhibition in rats following oral (gavage, dietary) and dermal exposures. The shaded tissues compartments indicate organs in which B-est (AChE, BuChE, and CaE) enzyme activity is described. Model parameter definitions: Qc cardiac output (l/h); Q_i, blood flow to "*i*" tissue (l/h), Ca, arterial blood concentration (µmol/l); Cao, arterial blood concentration of oxon (µmol/l); Cv, pooled venous blood concentration (µmol/l); Cv_i, venous blood concentration draining "*i*" tissue (µmol/l); Cv_io, venous blood concentration of oxon draining "*i*" tissue (µmol/l); SA, surface area of skin exposed (cm^2); K_P, skin permeability coefficient (cm/h); K_{zero}, zero-order (µmol/h) rate of absorption from diet; Fa, fractional absorption (%); KaS and KaI, first-order rate constants for absorption from compartments 1 and 2 (per hour); KsI, first-order rate constant for transfer from compartment 1 and 2 (per hour); K_e, first-order rate constant for elimination of metabolite from compartment 3; $K_{m(1–4)}$, Michaelis constant for saturable processes ([µmol/l]; $Vmax_{(1–4)}$, maximum velocity for saturable process (µmol/h). (B). Metabolic scheme for the metabolism of CPF and the major metabolites CPF-oxon, TCP, and conjugates (TCP), diethylphosphate and diethythiophosphate. Figure 1A adapted from Timchalk *et al.* (2002).

TABLE 1
Physiological Parameters, and Chemical Partitioning for CPF and CPF-oxon in the Preweanling and Adult Rat

Parameters	Value	Parameters	CPF	CPF-oxon
Tissues % of body weight[a]		Partition coefficients[b]		
Blood	6	Brain/blood	15.1	8.3
Diaphragm	0.03	Diaphragm/blood	3.6	2.3
Rapidly perfused	4	Fat/blood	228	119
Slowly perfused	78	Liver/blood	11.7	6.5
		Rapid perfused/blood	3.6	2.3
		Slowly perfused/blood	3.6	2.3
		Skin/blood	6	—
		Oral absorption[a]		
		KaS (stomach; per hour)	0.01	—
		KaI (stomach; per hour)	0.5	—
		KsI (stomach; per hour)	0.5	—
		Blood flows		
		Cardiac output (l/kg/h)[a]		
		% of cardiac output[a]		
	15			
Diaphragm	0.6	Rapidly perfused		42.6
Fat	9	Slowly perfused		14
Liver	25	Skin		5.8

Note. The model parameters were estimated independently and held fixed, calculated, or fitted as previously described (Timchalk *et al.*, 2002).

[a]Timchalk *et al.* (2002).

[b]Lowe *et al.* (2006).

based on the ratio of AChE activity in brain and RBC as previously described (Timchalk *et al.*, 2002). These estimates of tissue ChE and CaE levels were used in the PBPK/PD model to establish steady-state enzyme levels (μmol) and to enable calculation of the relative extent of enzyme inhibition as a function of CPF-oxon concentration in the various tissue compartments. These calculated changes in the plasma B-est (CaE, AChE and BuChE) levels (μmol) as a function of age in the rat are presented in Figure 3B. Similar analyses were conducted for the brain, diaphragm, and liver (data not shown). The enzyme degradation (K_d) rates for AChE, BuChE, and CaE were initially based upon the first-order loss of rat brain AChE as described by Gearhart *et al.* (1990). In general, BuChE activity is similar to AChE and as a first approximation the synthesis and loss rates for BuChE were set the same as for AChE. Whereas for CaE, reasonable parameter estimates for synthesis and loss rates were not available so the rates were optimized with the PD model to fit CaE inhibition data from Chanda *et al.* (1997; Timchalk *et al.*, 2002). For example, the equations describing AChE inhibition in the brain are

$$\frac{\mathrm{dBChE}}{\mathrm{d}t} = K_s - \mathrm{BChE} \times (K_d + K_i \times \mathrm{CBo}) + \mathrm{Inactive} \times K_r,$$

$$\mathrm{BChE} = \int_{\mathrm{IBChE}}^{t} \mathrm{dBChE}\,\mathrm{d}t,$$

$$\frac{\mathrm{dInactive}}{\mathrm{d}t} = \mathrm{BChE} \times K_i \times \mathrm{CBo} - \mathrm{Inactive} \times (K_a + K_r),$$

$$\mathrm{Inactive} = \int_{0}^{t} \mathrm{dInactive}\,\mathrm{d}t,$$

$$\mathrm{IBChE} = \frac{\mathrm{Best_l}}{\mathrm{EnzTurnover}},$$

TABLE 2
Scaling Equations used to Calculate Age-Dependent Changes in Organ Volumes and Metabolism in Preweanling and Adult Rats

Parameter	Equation
Body weight (Bwt)	$\mathrm{Bwt} = (-1E^{-8} \times \mathrm{AGE}^4) + (5E^{-7} \times \mathrm{AGE}^3) + (8E^{-5}*\mathrm{AGE}^2) + (0.001 \times \mathrm{AGE}) + 0.0101$
Liver % of body weight (%)	$\% = (4E^{-8} \times \mathrm{AGE}^4) - (6E^{-6} \times \mathrm{AGE}^3) + (0.0003 \times \mathrm{AGE}^2) - (0.0042 \times \mathrm{AGE}) + 0.0473$
Brain % of body weight (%)	$\% = (-5E^{-8} \times \mathrm{AGE}^4) + (7E^{-6} \times \mathrm{AGE}^3) - (0.0003 \times \mathrm{AGE}^2) + (0.0037 \times \mathrm{AGE}) + 0.0296$
Metabolic constants[a]	
CYP450 CPF to TCP	
K_m (μmol/l)	1.54[b]
$\mathrm{VmaxC_1}$ (μmol/h/kg)	273[c]
$\mathrm{VmSC_1}$ (scaling adjustment)	0.36[b]
$\mathrm{Vmax_1}$ (μmol/h)	$\mathrm{Vmax_1} = (\mathrm{VmSC_1} \times \mathrm{VmaxC_1}) \times \mathrm{Bwt}^{1.26}$
CYP450 CPF to oxon	
K_m (μmol/l)	0.23[b]
$\mathrm{VmaxC_2}$ (μmol/h/kg)	80[c]
$\mathrm{VmSC_2}$ (scaling adjustment)	0.28[b]
$\mathrm{Vmax_2}$ (μmol/h)	$\mathrm{Vmax_2} = (\mathrm{VmSC_2} \times \mathrm{VmaxC_2}) \times \mathrm{Bwt}^{1.68}$
PON-1 oxon to TCP (liver)	
K_m (μmol/l)	577[b]
$\mathrm{VmaxC_3}$ (μmol/h/kg)	38,002[d]
$\mathrm{VmSC_3}$ (scaling adjustment)	5[b]
$\mathrm{Vmax_3}$ (μmol/h)	$\mathrm{Vmax_3} = (\mathrm{VmSC_3} \times \mathrm{VmaxC_3}) \times \mathrm{Bwt}^{1.68}$
PON-1 oxon to TCP (blood)	
K_m (μmol/l)	464[b]
$\mathrm{VmaxC_4}$ (μmol/h/kg)	40,377[d]
$\mathrm{VmSC_4}$ (scaling adjustment)	3[b]
$\mathrm{Vmax_4}$ (μmol/h)	$\mathrm{Vmax_4} = (\mathrm{VmSC_4} \times \mathrm{VmaxC_4}) \times \mathrm{Bwt}^{1.96}$

[a]Scaling algorithm based upon the age-dependent CYP450 and PON-1 metabolism reported by Atterberry *et al.* (1997).

[b]Optimized parameter.

[c]Ma and Chambers (1994).

[d]Mortensen *et al.* (1996).

$$\mathrm{Best_l} = \mathrm{BestC_l} \times \mathrm{Bwt}^{0.7}$$

$$\%\mathrm{Activity} = \frac{\mathrm{BChE}}{\mathrm{IBChE}} \times 100$$

where *dBChEdt* is the rate of change (μmol/h) of brain AChE enzyme; K_s is the zero-order enzyme synthesis rate (μmol/h); BChE is the amount (μmol) of available enzyme; K_d, K_r, and K_a are the first-order rates (/h) for enzyme degradation, regeneration, and aging, respectively; K_i (μM h)$^{-1}$ is the bimolecular inhibition rate constant; and CBo is the concentration (μmol/l) of CPF-oxon in the brain. "Inactive" is the amount (μmol) of AChE that is inactive due to phosphorylation of the enzyme, and IBChE is the initial brain AChE concentration. The percent (%) of enzyme activity is expressed as the ratio between the amount of available enzyme (BChE) and the initial levels (IBChE).

TABLE 3
Parameters Used in the PD Model for CPF-Oxon Inhibition of AChE, BuChE, and CaE in Preweanling and Adult Rats

Parameters	Turnover rate[a] (μmol substrate per hour/μmol active site)
AChE	1.17 E^{+7}
BuChE	3.66 E^{+6}
CaE	1.09 E^{+5}

Parameters	Enzyme degradation rates (/h)	Enzyme reactivation rates (/h)	Enzyme aging rates (/h)	Bimolecular inhibition K_i (μM h)$^{-1}$
AChE				
Brain, diaphragm, liver[b], plasma[b]	0.01	0.014	0.0113	Scaled[c]
RBC	0.008	0.072[a]	0.0113	Estimated[c]
BuChE				
Brain, diaphragm, liver[b], plasma[b]	0.01	0.014	0.0113	2000
CaE				
Brain	7.54 E^{-4}	0.014	0.0113	20
Diaphragm, liver	0.001	0.014	0.0113	20
Plasma	0.0033	0.016	0.0113	20

Note. The model parameters were estimated independently and held fixed, calculated, or fitted as previously described (Timchalk *et al.*, 2002).

[a]Maxwell *et al.* (1987).

[b]Parameter estimates have been updated from published value in Timchalk *et al.* (2002), and are currently used to fit experimental results in both the adult and neonatal PBPK/PD models.

[c]See Table 4.

Those PBPK/PD model parameters that were modified as a function of age or changed relative to the adult model (Timchalk *et al.*, 2002) are presented in Table 4. Since there was no information on the extent of oral CPF absorption in preweanling pups, it was set at 100% for all ages. The percentage of body fat in the pups was based on an extrapolation of age-dependent changes in fat reported for the Sprague–Dawley rat (Schoeffner *et al.*, 1999). The fractional binding of CPF and CPF-oxon with blood proteins was both set at 95% based upon recently reported results (Lowe *et al.*, 2006), in both preweanling and adult rats which is slightly changed from the 97% to 98% binding used in the original adult model (Timchalk *et al.*, 2002). The brain AChE bimolecular inhibition rate constant (K_i) was measured *in vitro* at each postnatal age and was shown to decrease with age (Kousba *et al.*, 2007). The experimentally determined K_i was applied to the brain, plasma, liver, and diaphragm compartments. However, the K_i for the RBC AChE was initially based upon the parameter estimate in the previous PBPK/PD model (Timchalk *et al.*, 2002), and was proportionally scaled based on the measured age-dependent changes reported by Kousba *et al.* (2007). The K_i's for BuChE and CaE inhibition were not determined experimentally, so these parameter estimates were also based on the previously published model (Timchalk *et al.*, 2002).

Sensitivity analysis. A sensitivity analysis was conducted using the subroutines within acslXtreme to identify the importance of selected parameters relative to their impact on brain AChE inhibition response. This analysis primarily focused on those model parameters that substantially changed as a function of age. The sensitivity of the model to these parameters was assessed for simulations at postnatal days (PND)-5, PND-17 (data not shown), and in adult rats following a single oral gavage dose of 5 mg/kg of body weight. The 5 mg/kg dose was selected since model simulations (see "PND-5 vs. Adult Oxon Area Under Concentration Curve (AUC)") suggest that the brain CPF-oxon concentration was disproportionately increased in PND-5 relative to adult rats at this dose level. The analysis measured a change in model output (brain AChE) corresponding to a 1% change in the parameter of interest (e.g., Vmax) when all other parameters were held fixed. Sensitivity parameters were qualitatively categorized as having low, medium, or high uncertainty based on the following criteria: low, experimental data obtained in the rat in our laboratory or from the published literature; medium, scaled value from a different species or optimized based on multiple data sets; high, parameters optimized from limited data or lacking published or historical values. These criteria are similar to those utilized by Teeguarden *et al.* (2005) for ranking uncertainty of model parameter estimates (see supplemental data file 10 for additional detail).

RESULTS

In order to adequately address age-dependent changes in both the pharmacokinetics of CPF and the resulting PD (i.e., ChE) response, a number of metabolic and physiological parameters were scaled as a function of age. The initial evaluation focused on the capability of the updated model to adequately simulate blood CPF and CPF-oxon dosimetry in the adult rat and the results from these comparisons are presented in Figure 4. In general the model adequately simulated the available CPF blood concentrations at doses ranging from 1 to 50 mg/kg (data from Timchalk *et al.*, 2002). In addition, although CPF-oxon was only detectable in a very limited number of blood samples (peak concentrations at 10 and 50 mg/kg) the model also provided a reasonable simulation of these data. Since CPF-oxon is responsible for the observed ChE inhibition, the good fits for blood and brain ChE inhibition (see Figs. 7 and 9) in the adult rat also suggest that the model reasonably predicts CPF-oxon blood and tissue concentrations. These model simulations include a number of updated model parameters (Kousba *et al.*, 2004, 2007; Lowe *et al.*, 2006; Poet *et al.*, 2003) and show a slightly improved fit to the experimental data relative to the previously published model (Timchalk *et al.*, 2002).

Pharmacokinetics of CPF and TCP

The experimentally determined time-course of CPF and TCP in blood of preweanling rats (PND-5, -12, and -17) following oral gavage administration of CPF at doses of 1 or 10 mg/kg body weight (Timchalk *et al.*, 2006), and model simulations (solid lines) of these experimental data are presented in Figure 5. Both the data and model simulations suggest that CPF is rapidly absorbed and metabolized since peak blood levels of both CPF and the major metabolite TCP were observed between 3- and 6-h postdosing. Within all age groups a comparison of the measured maximum blood concentration (C_{max}) and the PBPK model predictions suggests that the kinetics of both CPF and TCP are linear over the dose range (1–10 mg/kg). The experimentally determined C_{max} for CPF is comparable across preweanling ages; whereas, the model predicts a consistently lower C_{max} at both doses and ages, and also suggests a decreasing trend with

TABLE 4
Modified Parameters used in the Age-Dependent PBPK/PD model for CPF and CPF-oxon to describe Dosimetry, Metabolism, and ChE Inhibition Dynamics in Preweanling and Adult Rats

	Age (days)				
Parameter	5	12	17	Adult	Estimation method[a]
Fractional absorption (%)	100	100	100	100	Fixed
% of body weight					
Fat (%)	3	5	7	7	Fixed[b]
% of cardiac output					
Brain (%)	7	7	7	3	Fixed[c]
Plasma protein binding					
CPF (%)	95	95	95	95	Fixed[d]
CPF-oxon (%)	95	95	95	95	Fixed[d]
TCP model parameters					
Vd (l)	0.007	0.012	0.007	—	Fitted
Elimination rate K_e (/h)	0.15	0.15	0.15		Fitted
Bimolecular inhibition rate $(\mu M\ h)^{-1}$					
Tissues AChE (plasma, brain, diaphragm, liver)	950[e]	500[e]	220[e]	243[f]	Measured
RBC AChE	431	227	100	100	Fixed
B-est$_{(1-12)}$ enzyme activity (μmol/h)[h]					
AChE					
Brain B-estC$_1$ (μmol/h/kg)		3487			Calculated[f,g]
B-est$_1$ (μmol/h)		B-est$_1$ = B-estC$_1$ × Bwt$^{0.7}$			
Diaphragm B-estC$_2$ (μmol/h/kg)		21			Calculated[f,g]
B-est$_2$ (μmol/h)		B-est$_2$ = B-estC$_2$ × Bwt$^{0.83}$			
Hepatic B-estC$_3$ (μmol/h/kg)		323			Calculated[f,g]
B-est$_3$ (μmol/h)		B-est$_3$ = B-estC$_3$ × Bwt$^{0.83}$			
Plasma B-estC$_4$ (μmol/h/kg)		5230[i]			Calculated[f,g]
B-est$_4$ (μmol/h)		B-est$_4$ = B-estC$_4$ × Bwt$^{0.83}$			
BuChE					
Brain B-estC$_5$ (μmol/h/kg)		371			Calculated[f,g]
B-est$_5$ (μmol/h)		B-est$_5$ = B-estC$_5$ × Bwt$^{1.3}$			
Diaphragm B-estC$_6$ (μmol/h/kg)		5.2			Calculated[f,g]
B-est$_6$ (μmol/h)		B-est$_6$ = B-estC$_6$ × Bwt$^{0.76}$			
Hepatic B-estC$_7$ (μmol/h/kg)		950			Calculated[f,g]
B-est$_7$ (μmol/h)		B-est$_7$ = B-estC$_7$ × Bwt$^{0.76}$			
Plasma B-estC$_8$ (μmol/h/kg)		618			Calculated[f,g]
B-est$_8$ (μmol/h)		B-est$_8$ = B-estC$_8$ × Bwt$^{0.76}$			
CaE					
Brain B-estC$_9$ (μmol/h/kg)		475			Calculated[f,g]
B-est$_9$ (μmol/h)		B-est$_9$ = B-estC$_9$ × Bwt$^{0.7}$			
Diaphragm B-estC$_{10}$ (μmol/h/kg)		63			Calculated[f,g]
B-est$_{10}$ (μmol/h)		B-est$_{10}$ = B-estC$_{10}$ × Bwt$^{0.7}$			
Hepatic B-estC$_{11}$ (μmol/h/kg)		61,563			Calculated[f,g]
B-est$_{11}$ (μmol/h)		B-est$_{11}$ = B-estC$_{11}$ × Bwt$^{0.7}$			
Plasma B-estC$_{12}$ (μmol/h/kg)		18,051			Calculated[f,g]
B-est$_{12}$ (μmol/h)		B-est$_{12}$ = B-estC$_{12}$ × Bwt$^{0.7}$			

[a]The model parameters were estimated independently and held fixed (fixed), measured in independent experiments (measured), calculated utilizing mathematical algorithms (calculated), or estimated by fitting the model to the data (fitted).
[b]Schoeffner *et al.* (1999).
[c]Gentry *et al.* (2004).
[d]Lowe *et al.* (2006).
[e]Kousba *et al.* (2007).
[f]Timchalk *et al.* (2002).
[g]Maxwell *et al.* (1987).
[h]Scaling algorithms based upon the age-dependent changes in tissue AChE, BuChE, and CaE enzyme activity as determined by Atterberry *et al.*(1997), Tang *et al.* (1997), Mortensen *et al.* (1998), and Carr *et al.* (2001).
[i]Fixed (10x)

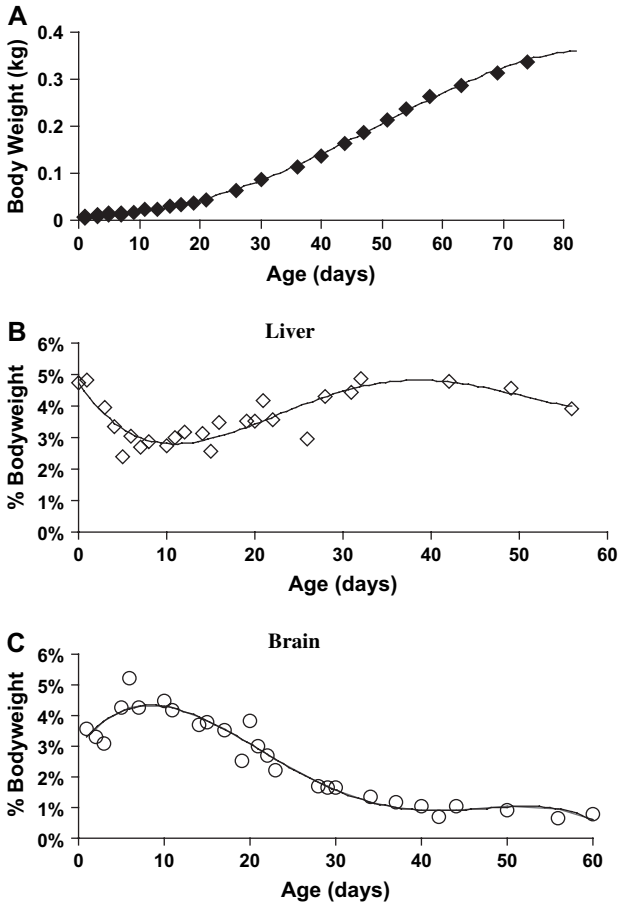

FIG. 2. Age-dependent scaling of (A) body weight (kg); (B) liver volume (% of body weight); and (C) brain volume (% of body weight) as a function of age in Sprague–Dawley rats. Body weight data obtained from Carr *et al.* (2001) and Charles River Laboratory. The liver and brain data were obtained from Gentry *et al.* (2004)

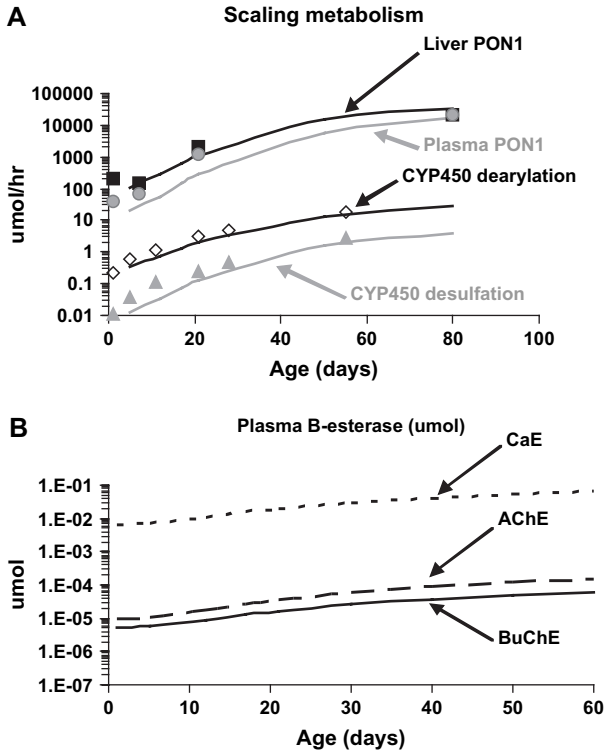

FIG. 3. (A) Scaling of metabolic rates as a function of age for hepatic and plasma PON-1, and hepatic CYP450 mediated dearylation and desulfation of CPF and CPF-oxon in the rat. Symbols represent experimentally determined enzyme activity (Atterberry *et al.*, 1997); whereas, lines represent model prediction; and (B) scaling of the amount of plasma B-est (CaE, AChE, and BuChE) as a function of age in the rat, similar scaling was done for hepatic, diaphragm, and brain B-est levels (data not shown).

age. Of interest to note is that the model underpredicts the CPF blood concentration, particularly in PND-12 and -17 rats and simulates a faster blood elimination relative to the experimental data. With regard to the blood TCP kinetics, in PND-5 and -12 rats the blood time-course and C_{max} (observed and predicted) for TCP are very comparable, and both the experimental data and model predictions increase ~3-fold at both dose levels in the PND-17 rats.

Domoradski *et al.* (2004) compared the pharmacokinetics of CPF and TCP in PND-5 rats following exposure by different routes (oral vs. subcutaneous), formulations (corn oil vs. milk vs. dimethylsulfoxide), and rates (single bolus vs. fractionated) of administration. The time-course of CPF and TCP in blood following a single oral bolus 1 mg CPF/kg body weight dose in corn oil or as three fractionated doses of 0.33 mg/kg each in PND-5 rats is presented in Figure 6. In this experiment, a substantial number of blood concentration time-points for both CPF and TCP were determined. Peak blood concentrations of CPF and TCP were attained at 3- to 6-h postdosing (Fig. 6A). Compared to the results seen in Figures 5A and 5D the C_{max} for CPF was slightly higher (0.14 vs. 0.07 μmol/l) while the blood TCP concentration was lower (1.61 vs. 3.85 μmol/l); however, the overall pharmacokinetic profile was very comparable and the PBPK/PD model reasonably simulated the CPF and TCP blood time-course. Likewise the model reasonably simulated the CPF and TCP blood time-course following the split dose exposure experiment (Fig. 6B). As anticipated, the C_{max} for CPF and TCP following the fractionated CPF doses were lower (2.8–7.4 fold) than following the single bolus administration and the PBPK/PD model reasonably simulated this response.

PD of ChE Inhibition

The PBPK/PD model (Timchalk *et al.*, 2002) developed to describe the CPF-oxon stoichiometric inhibition of both target (i.e., AChE) and nontarget B-est (i.e., CaE and BuChE) was adapted to incorporate age-dependent parameter estimates. Parameter estimates and scaling equations for the PD model are presented in Tables 3 and 4. In the current model, the tissue B-est enzyme levels were scaled as a function of age (see Fig. 3B), and the measured K_i for AChE in PND-5, -12, and -17

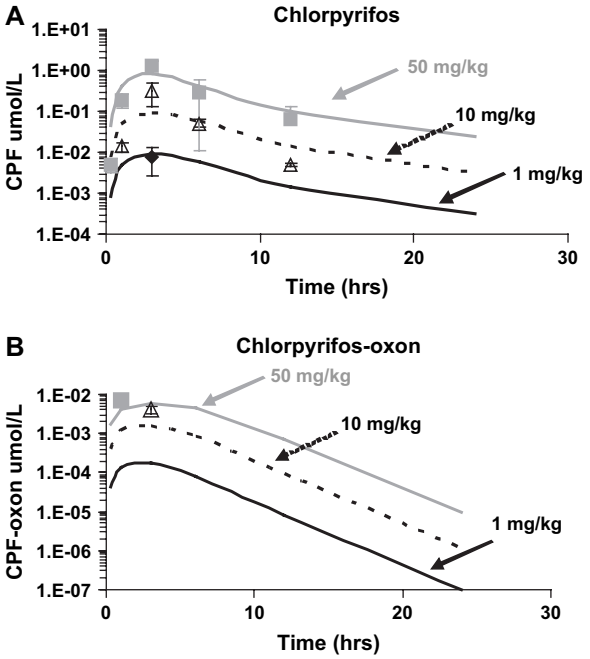

FIG. 4. PBPK/PD model simulations of (A) CPF and (B) CPF-oxon blood concentrations, in adult rats following single oral gavage doses of 1, 10, or 50 mg CPF/kg of body weight. The lines represent the model simulations utilizing the age-dependent PBPK/PD model; the experimental data were obtained from Timchalk *et al.* (2002).

rats of 950, 500, and 220 $(\mu M\ h)^{-1}$, respectively, were applied (Kousba *et al.*, 2007). The K_i for RBC AChE in the adult model was set at 100 $(\mu M\ h)^{-1}$, while in the current model the RBC AChE K_i for PND-5 and -12 rats was proportionally adjusted to 431 and 227 $(\mu M\ h)^{-1}$, respectively, based on changes reported by Kousba *et al.* (2007) with brain AChE. The CaE and BuChE K_i values and the reactivation (K_r) and aging (K_a) rates for the B-est were based on the previously published model (Timchalk *et al.*, 2002).

The time-courses of plasma ChE, RBC AChE, and brain AChE inhibition were previously determined (Timchalk *et al.*, 2002, 2006) in the preweanling (PND-5 to PND-17) and adult (plasma and brain only) rats through 24-h postdosing following single oral gavage administration of CPF at doses of 1 or 10 mg/kg and along with the PBPK/PD model predictions (solid lines) are presented in Figures 7–9. In these experiments, CPF produced a dose- and age-dependent (i.e., younger more sensitive) inhibition of tissue B-est activity.

Plasma ChE Inhibition

For both doses, the maximum plasma ChE inhibition (MaxI) expressed as the percentage of control activity and PBPK/PD model simulations increased as a function of age such that the extent of ChE inhibition in preweanling rats followed the pattern PND-5 > PND-12 > PND-17 (see Figs. 7A–C). Maximum inhibition at the low dose was achieved by ~3-h postdosing, and ~6 h at the high dose; recovery of enzyme activity was marginal through 24 h. As noted in the Methods section, to more reasonably fit the overall plasma ChE response at all ages the basal plasma AChE activity reported by Maxwell *et al.* (1987) was increased by a factor of 10. With this modification the PBPK/PD model consistently simulated the maximum ChE inhibition at ~6-h postdosing, and model simulation of enzyme recovery through 24-h postdosing was consistent with the experimental data. For adult rats administered the same doses (see Fig. 7D) the maximum plasma ChE inhibition was comparable to the response seen in PND-12 and -17 rats. Overall, these results indicate that the PD model provided a reasonable simulation of the age- and dose-dependent inhibition of plasma ChE activity in the neonatal and adult rats.

RBC AChE Inhibition

As illustrated in Figure 8, the experimental result time-course of RBC AChE also demonstrated an age- and dose-dependency in preweanling rats with the extent of inhibition following the pattern PND-5 > PND-12 > PND-17 at both doses (Timchalk *et al.*, 2006). The PBPK/PD model (solid lines) accurately simulated both the dose- and age-dependent RBC AChE inhibition through 24-h postdosing. Although the timing to maximal inhibition of RBC AChE (3- to 6-h postdosing) was very comparable to the response seen with plasma ChE, consistent with previous observations in rats (Timchalk *et al.*, 2002) the magnitude of the RBC AChE inhibition as reflected by both the experimental data and model simulations was less than for the plasma ChE at all ages.

Brain AChE Inhibition

The time-course for brain AChE inhibition (Timchalk *et al.*, 2002, 2006) and model simulations are presented in Figure 9 and are similar to the responses seen with plasma ChE and RBC AChE. The experimentally determined time-course of brain AChE inhibition demonstrated both an age- and dose-dependency in the preweanling rats (Timchalk *et al.*, 2006), and at all dose levels and ages the PBPK/PD model reasonably simulated the dynamics of brain AChE inhibition (Fig. 9). At a dose of 1 mg/kg only the PND-5 rats exhibited any brain AChE inhibition (MaxI, 78% of control); whereas, no inhibition was noted in PND-12 and -17 rats as compared with the controls. In contrast, a dose of 10 mg/kg resulted in substantial inhibition of brain AChE at all preweanling ages with the experimentally determined MaxI at PND-5, -12, and -17 being 16%, 20%, and 41% of control, respectively. In adult rats administered 1 or 10 mg CPF/kg of body weight, measured brain AChE activity (MaxI) was 103% and 85% of control, respectively (see Fig. 8D). These results suggest that the adult rat brain AChE is fairly refractory to the CPF-oxon inhibition at a dose as high as 10 mg/kg; whereas, at all ages in the preweanling rats the enzyme activity was more substantially

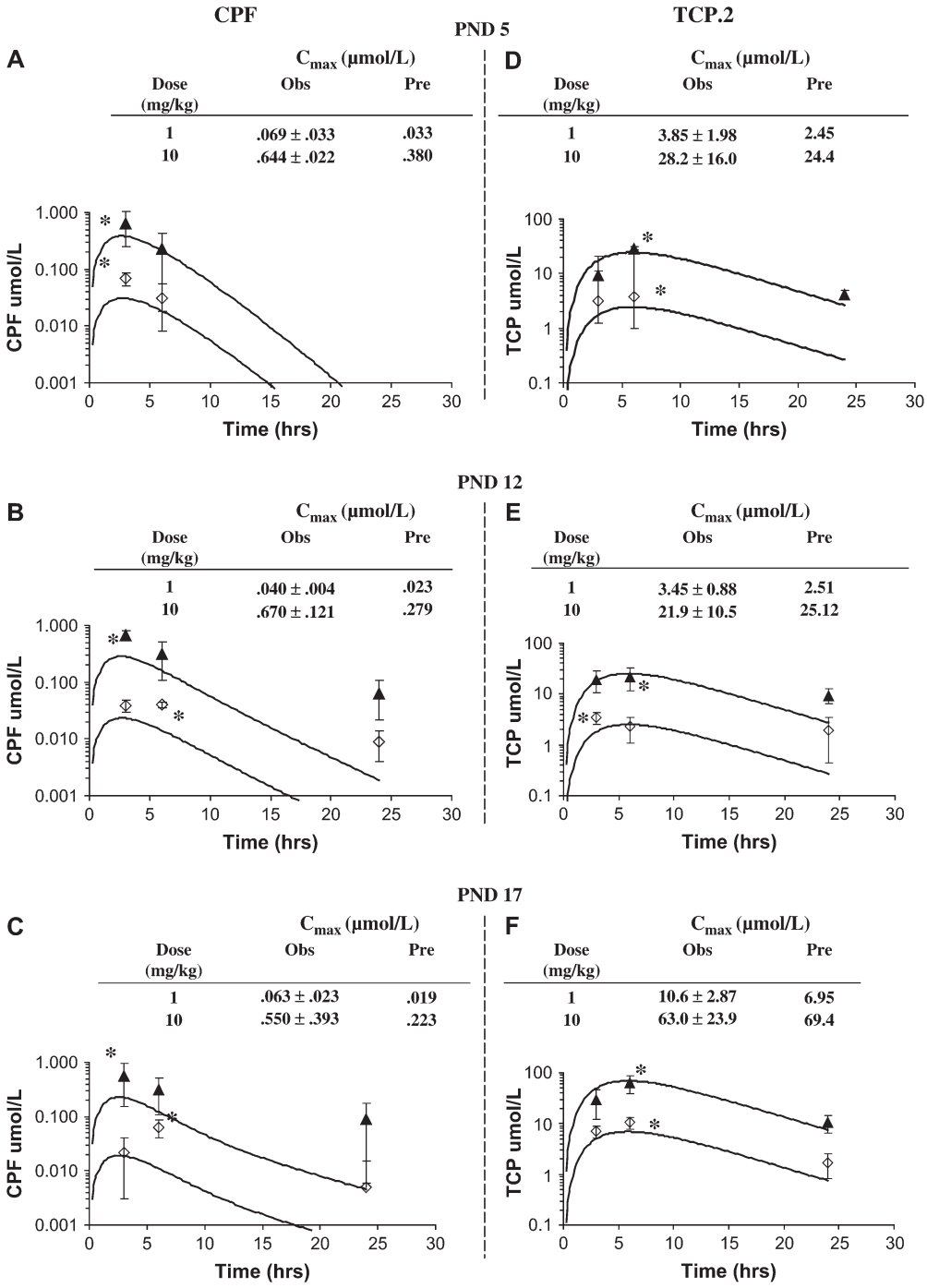

FIG. 5. Observed data and model prediction (line) for the blood time-course concentrations of CPF (A–C), and TCP (D–F) in postnatal day-5 (PND-5), PND-12, and PND-17 rats following a single acute oral gavage dose of 1 (open diamond) or 10 (closed triangle) mg CPF/kg of body weight. The observed (Obs) data are presented as a mean ± SD of four to five animals per time point. The * identifies the experimentally measured C_{max} time point and is presented in the table insert along with the corresponding model prediction (Pre). The observed data were obtained from Timchalk *et al.* (2006).

inhibited. This age- and dose-dependent response as reflected by both the experimental data and model simulations is consistent with the greater sensitivity of juvenile rats to the acute high-dose effects of CPF relative to adults (Moser and Padilla, 1998; Pope and Liu, 1997; Pope *et al.*, 1991).

Model Simulation of ChE Recovery

Since the previous study (Timchalk *et al.*, 2006) only evaluated CPF dosimetry and ChE inhibition through 24-h postdosing, the full recovery of ChE activity was not

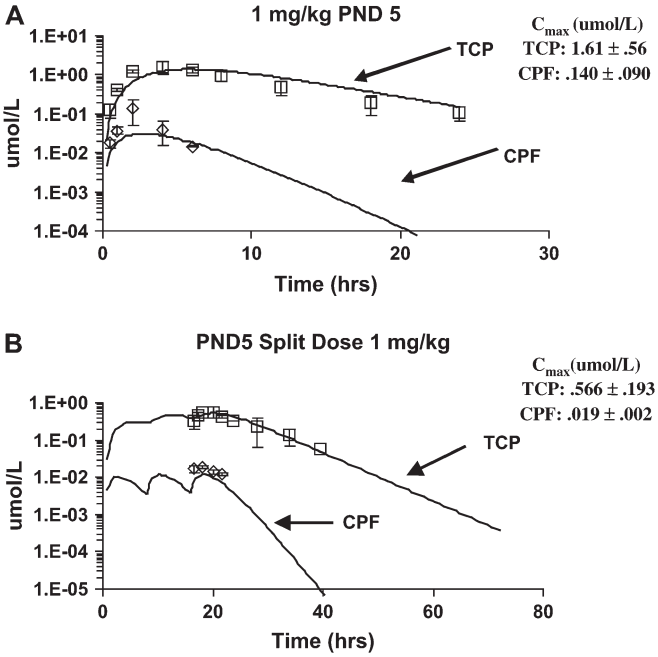

FIG. 6. Observed data and model prediction (line) for blood concentrations of CPF and TCP in PND-5 rats given (A) a single oral gavage dose of 1 mg/kg; or (B) three split doses of 0.33 mg/kg each administered at 0, 8, and 16 h. The observed data are a mean ± SD of four to five animals per time point. The C_{max} is the maximally measured blood concentration. The observed data were obtained from Domoradski *et al.* (2004).

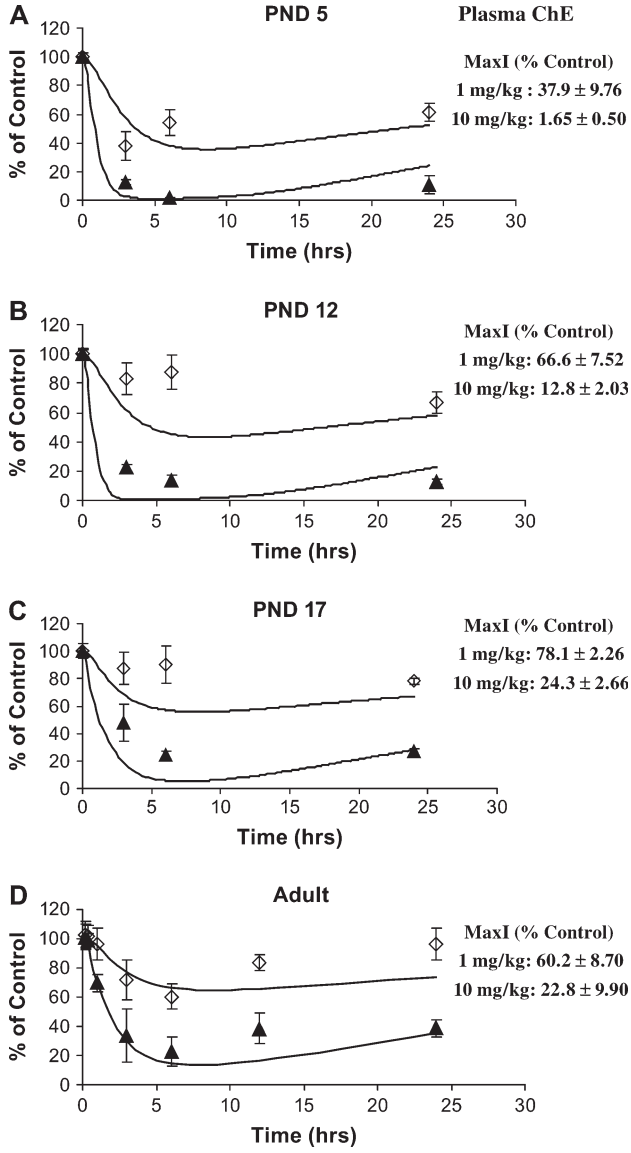

FIG. 7. Observed data and model prediction (line) for the plasma ChE inhibition time-course in (A) postnatal day-5 (PND-5); (B) PND-12; (C) PND-17; and (D) adult rats following a single acute oral gavage dose of 1 (open diamond) or 10 (closed triangle) mg CPF/kg of body weight. The observed data are presented as a mean ± SD of four to five animals per time point. The MaxI is expressed as % of control activity for each of the dose levels. The neonatal and adult data were obtained from Timchalk *et al.* (2002, 2006).

observable. To evaluate the capability of the model to simulate recovery of ChE activity the model simulation was compared against several different published data sets. Won *et al.* (2001) evaluated the extent of brain (frontal cortex) AChE inhibition through 96-h postdosing following oral gavage administration of CPF at doses corresponding to the LD_{10} and 50% of the LD_{10} in neonatal (PND-7: 15 and 7.5 mg/kg), juvenile (PND-21: 47 and 23.5 mg/kg), and adult (PND-90: 136 and 60 mg/kg) Sprague–Dawley rats (see Fig. 10). The low and high doses were anticipated to produce comparable responses across ages, and the authors reported that the brain AChE inhibition ranged from 40% to 60% (50% LD_{10}) and 80% to 90% (LD_{10}), respectively (Won *et al.*, 2001). As illustrated in Figure 10, the PBPK/PD model simulations (solid lines) did result in comparable brain AChE inhibition for all ages, consistent with the experimental design (50% and 100% of LD_{10}). However, in PND-7 rats the model overpredicted the observed inhibition following the low dose (7.5 mg/kg), and in adults the model-predicted brain AChE recovery was slightly faster than the observed response at 24- and 96-h postdosing for both dose levels (68 and 136 mg/kg). Nonetheless, the model simulations are reasonably consistent with the observed experimental data and experimental design.

Moser and Padilla (1998) likewise evaluated the toxicity of CPF in male and female PND-17 Long Evans rats that were orally administered CPF by gavage at a maximum tolerated dose of 15 mg/kg. In this study the time-course of brain and RBC AChE activity were determined through 14 days (336 h) postexposure. The results of the model simulations for both brain and RBC AChE are presented in Figure 11. Moser and Padilla (1998) reported average body weights for PND-17 male and female Long Evans rats as 34 and 33 g, respectively; which is consistent with the 33g predicted using the polynomial equation developed for Sprague–Dawley rats (see Table 2, Fig. 2A). In brains analyzed from both genders, the AChE time-course was very comparable and the maximum measured

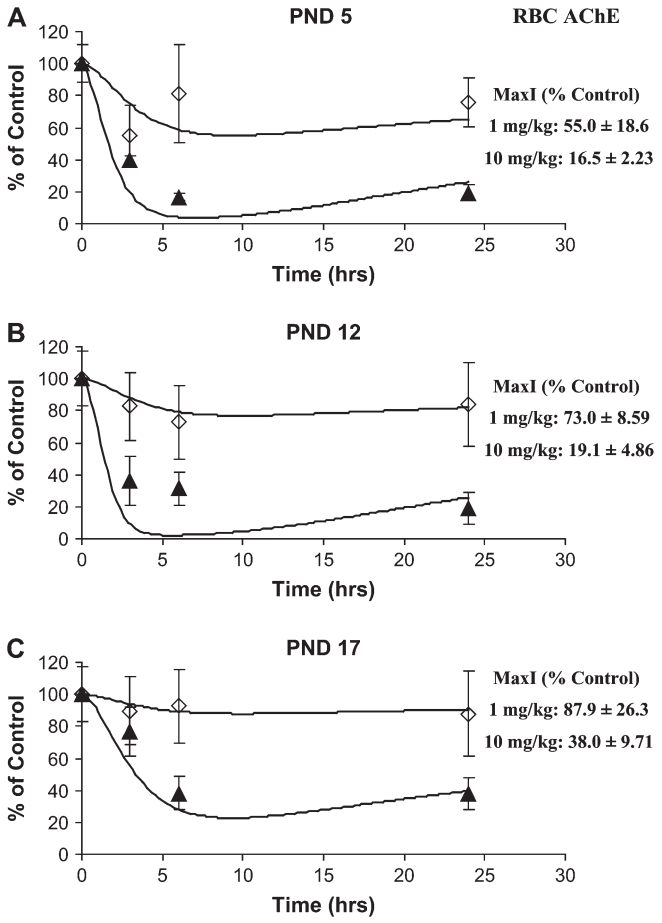

FIG. 8. Observed data and model prediction (line) for the RBC AChE inhibition time-course in (A) postnatal day-5 (PND-5); (B) PND-12; and (C) PND-17 rats following a single acute oral gavage dose of 1 (open diamond) or 10 (closed triangle) mg CPF/kg of body weight. The observed data are presented as a mean ± SD of four to five animals per time point. The MaxI is expressed as % of control activity for each of the dose levels. The observed data were obtained from Timchalk *et al.* (2006).

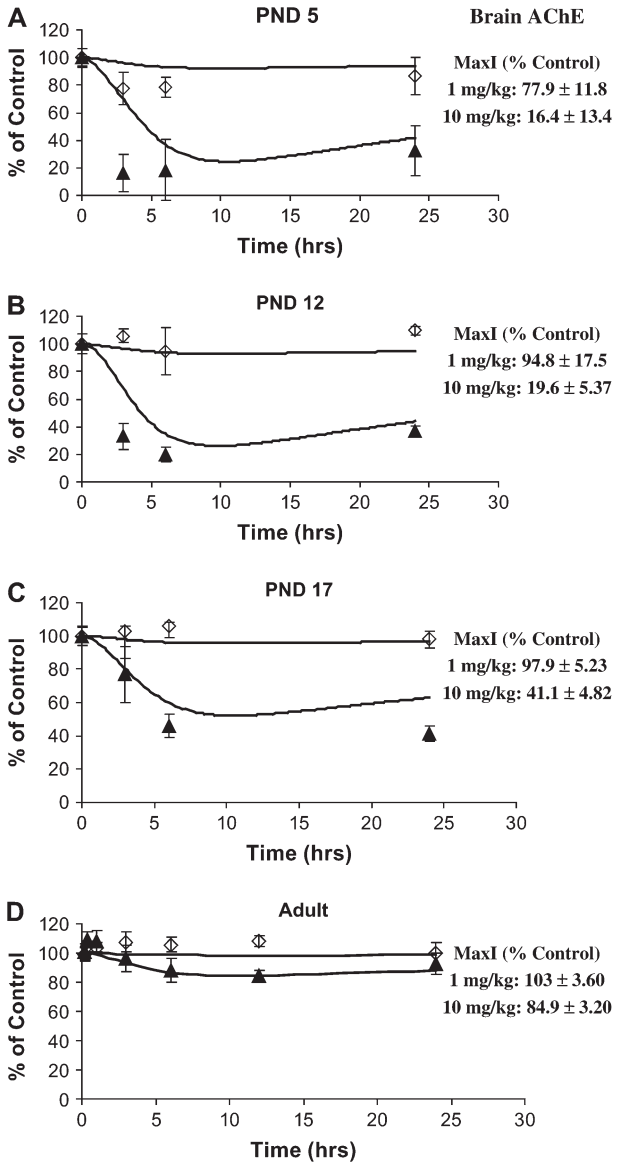

FIG. 9. Observed data and model prediction (line) for the brain AChE inhibition time-course in (A) postnatal day-5 (PND-5); (B) PND-12; (C) PND-17; and (D) adult rats following a single acute oral gavage dose of 1 (open diamond) or 10 (closed triangle) mg CPF/kg of body weight. The observed data are presented as a mean ± SD of four to five animals per time point. The MaxI is expressed as % of control activity for each of the dose levels. The neonatal and adult data were obtained from Timchalk *et al.* (2002, 2006).

AChE inhibition was ~11% of control (6-h postdosing) which recovered to ~80% by 162-h postdosing. Model simulations of these data resulted in a maximum inhibition of ~27% of control which was nearly fully recovered (~95%) by 160 h. Although the model predicted less inhibition than was experimentally observed, the simulations accurately reflected the enzyme recovery rate. With regard to RBC AChE, enzyme activity was significantly inhibited to 3–5% of control activity for both genders by ~6-h postdosing, which was very consistent with the model's maximum prediction of ~8% of control activity. However, the overall RBC AChE recovery rate appeared to be slightly faster in the females than in males, with the model predicting near maximal recovery by 160-h postdosing, which was consistent with the female data set. It is of interest to note that an improved fit to the experimental data (dashed line) could be obtained by allowing the model to optimize the fit to the experimental data by increasing the administered dose of CPF. By fitting the maximum inhibition, particularly for the brain AChE, the model provided a better fit of the overall brain AChE recovery profile through 350-h postdosing. However, the same approach for RBC AChE did not provide any substantial improvement.

ChE Inhibition for Single and Repeat CPF Oral Doses

Zheng *et al.* (2000) evaluated the age-dependent changes in neurochemical indicators of toxicity including brain AChE over a broad range of acute and repeated dose exposures to CPF

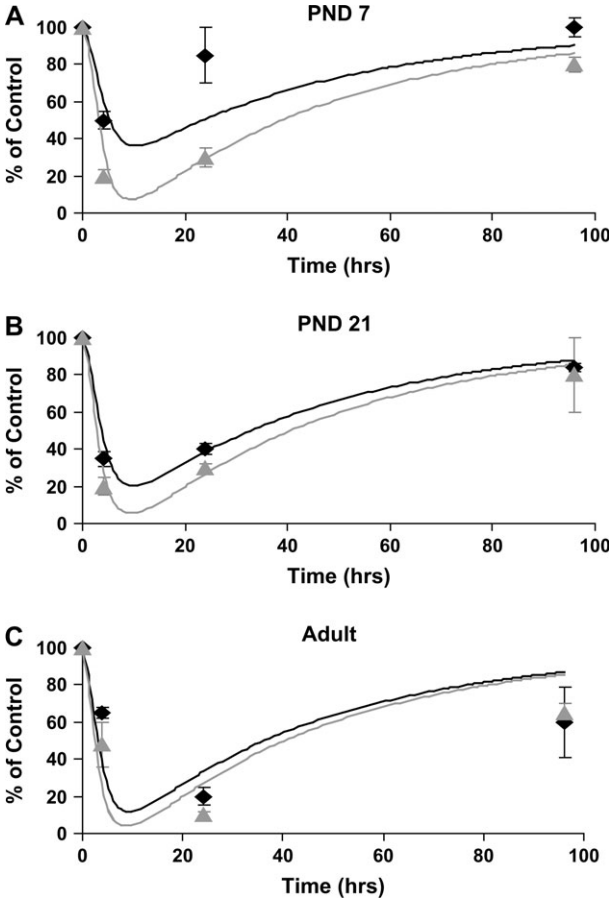

FIG. 10. Observed data and model prediction (line) for brain AChE inhibition time-course following single oral gavage doses of CPF. Doses were selected to give equal AChE inhibition responses. (A) PND-7 rats; doses 7.5 (black) and 15 (gray) mg/kg; (B) PND-21 rats; doses 23.5 (black) and 47 (gray) mg/kg; and (C) adult; doses 68 (black) and 136 (gray) mg/kg. The observed experimental data were extracted from Won *et al.* (2001).

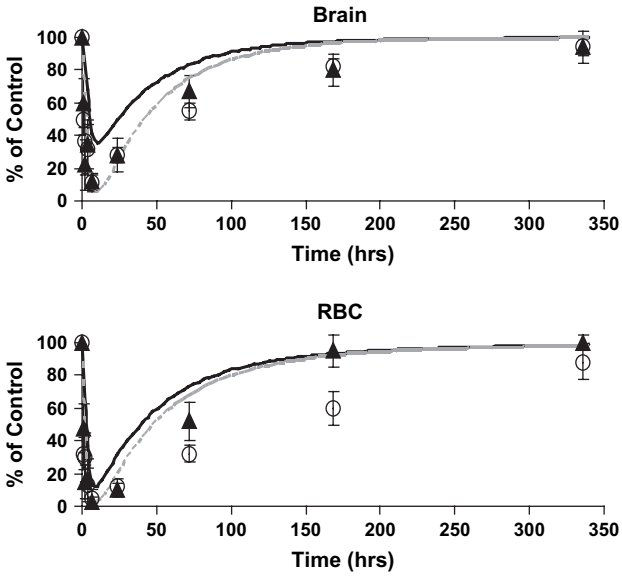

FIG. 11. Observed data and model prediction (line) for (A) brain and (B) RBC AChE inhibition time-course in male (open circles) and female (triangles) PND-17 rats following a single acute oral gavage dose of 15 mg chlropyrifos/kg of body weight. The gray dashed line is a simulation that optimized the dose to fit the experimental data. The observed data were extracted from Moser and Padilla (1998).

in PND-7 and -21 Sprague–Dawley rats. Beginning on PND-7, groups of rats were given either a single or 14 daily oral gavage doses, and sacrificed 4 h after the first or 14th dose, respectively. The inhibition of plasma ChE, RBC AChE, and brain AChE was evaluated and the observed and model-predicted response (single and repeat) is presented in Table 5 and the simulation of the 14 daily repeat doses is illustrated in Figure 12. As reported by Zheng *et al.* (2000) the observed dose-dependent plasma ChE and brain AChE inhibition was comparable for both the PND-7 and -21 animals that received either a single or repeated administration of CPF. In contrast, repeated CPF doses resulted in a greater RBC AChE inhibition (10–38%) at all dose levels relative to the single dose (Table 5, B). The PBPK/PD model accurately simulated the plasma ChE inhibition in PND-7 rats following single oral exposures ranging from 0.15 to 1.5 mg/kg. However, the lack of a dose–response for plasma ChE at doses $\geq$ 4.5 mg/kg resulted in the model overpredicting the amount of inhibition at these higher doses. The model also overpredicted the plasma ChE inhibition in PND-21 rats following the repeated exposure at all dose levels (Table 5, A). However, the model reasonably simulated the RBC AChE response following the single or repeated exposures (Table 5, B). The dose-dependent brain AChE inhibition was adequately simulated at doses ranging from 0.15 to 0.75 mg/kg, but was underpredicted at doses $\geq$ 1.5 mg/kg following the single (PND-7) exposures. The model tended to slightly underpredict the extent of brain AChE inhibition following the repeated (PND-21) doses, but the overall trend was consistent with the experimental results. Following repeated dose administration (see Figure 12) the time-course of plasma ChE, and RBC and brain AChE inhibition suggest that the maximum inhibition in plasma and RBC was achieved within two to four doses, whereas in the brain the maximum inhibition was not achieved until six to eight doses. It is also of interest to note that the brain AChE inhibition response was marginal at 0.75 mg/kg/day or less, but was substantially inhibited following repeated dosing > 1.5 mg/kg/day.

PND-5 versus Adult Oxon Area Under Concentration Curve

A comparison of the simulated CPF-oxon AUC ratios (PND-5 vs. adult) in both blood and brain over a broad range of CPF doses is illustrated in Figure 13. At doses ranging from 0.001 to 1 mg/kg the neonatal to adult CPF-oxon ratio [PND − 5 (AUC)]/Adult(AUC) for blood and brain were ~1.3; however, at CPF doses > 1 mg/kg the ratio rapidly increased in both blood and brain and approached 2 at ~10 mg/kg. This suggests that age-dependent difference in brain oxon concentration may

TABLE 5
Observed and Model-Predicted (A) Plasma ChE; (B) RBC AChE; and (C) Brain AChE Activity following a Single Oral Exposure to CPF in PND-7 Rats or following 14 Daily Repeated Exposures Starting at PND-7 through PND-21

	Single dose, age 7 days			Repeat dose, age 21 days		
A. Plasma ChE	% Activity 4-h postdosing			% Activity 4-h postdosing		
Dose (mg/kg)	Observed plasma	Predicted plasma	Predicted/ observed	Observed plasma	Predicted plasma	Predicted/ observed
0.15	90	89	0.99	90	75	0.83
0.45	72	70	0.97	80	55	0.69
0.75	62	55	0.89	78	41	0.52
1.5	50	32	0.64	42	22	0.53
4.5	22	5.5	0.25	22	3	0.14
7.5	20	1.8	0.09	15	1	0.07
15	22	0.7	0.03	—	—	—

	Single dose, age 7 days			Repeat dose, age 21 days		
B. RBC AChE	% Activity 4-h postdosing			% Activity 4-h postdosing		
Dose (mg/kg)	Observed RBC	Predicted RBC	Predicted/ observed	Observed RBC	Predicted RBC	Predicted/ observed
0.15	100	96	0.96	87	94	1.07
0.45	83	89	0.07	75	83	1.10
0.75	83	81	0.98	70	71	1.01
1.5	68	66	0.97	42	49	1.15
4.5	15	29	1.92	10	11	1.13
7.5	10	14	1.37	0	3	—
15	5	4	0.70	—	—	—

	Single dose, age 7 days			Repeat dose, age 21 days		
C. Brain AChE	% Activity 4-h postdosing			% Activity 4-h postdosing		
Dose (mg/kg)	Observed brain	Predicted brain	Predicted/ observed	Observed brain	Predicted brain	Predicted/ observed
0.15	100	99	0.99	100	98	0.98
0.45	100	98	0.98	90	94	1.05
0.75	100	96	0.96	80	89	1.11
1.5	80	92	1.15	58	75	1.29
4.5	20	76	3.80	20	26	1.31
7.5	17	63	3.70	12	6	0.50
15	15	39	2.60	—	—	—

Note. The experimental data were obtained from Zheng *et al.* (2000).

be an important contributing factor associated with the increased sensitivity of preweanling rats relative to adults particularly at the higher doses utilized in toxicology studies.

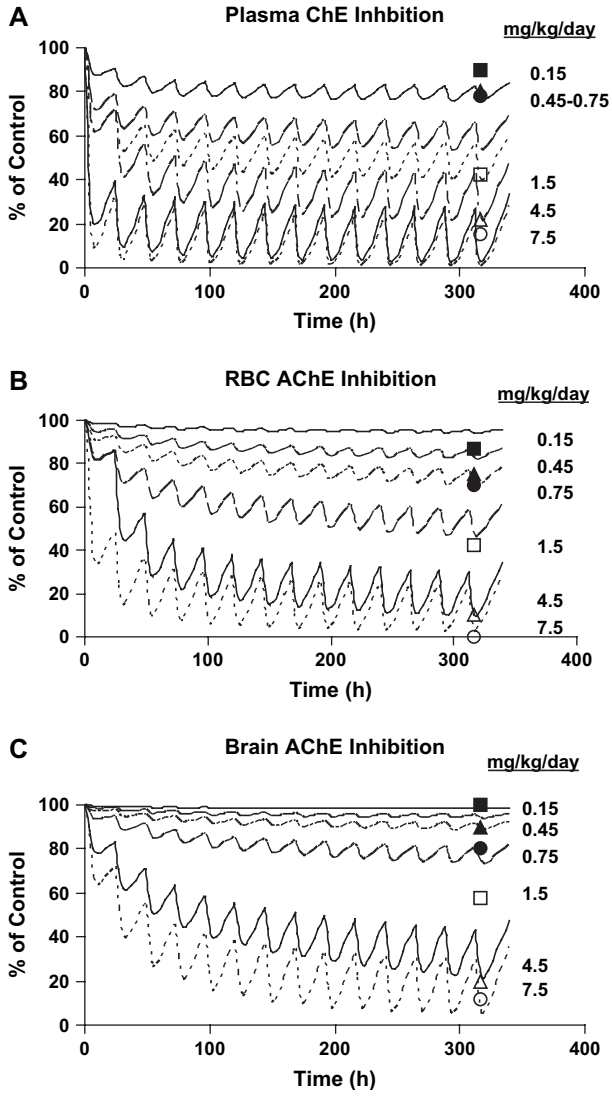

FIG. 12. Observed data and model prediction (line) for (A) plasma ChE; (B) RBC AChE; and (C) brain AChE inhibition time-course following 14 daily repeated exposures to CPF administered at doses of 0.15 (filled square), 0.45 (filled triangle), 0.75 (filled circle), 1.5 (open square), 4.5 (open triangle), and 7.5 (open circle) mg/kg/day beginning on PND-7 through PND-21. The esterase activity was determined in rats 4 h after the administration of the 14th dose. The experimental data were obtained from Zheng *et al.* (2000).

Sensitivity Analysis

A model sensitivity analysis was conducted to compare the relative impact of metabolism, brain AChE parameters, tissue volume changes, and blood flows on brain AChE response in PND-5 versus adult rats. A summary of these results is presented in Table 6 (acslXtreme®; see supplemental data). It was anticipated that hepatic metabolism and blood flow would most likely be important determinants of the extent of CPF-oxon formation and detoxification which could modify brain oxon dosimetry and associated AChE inhibition. In addition, the

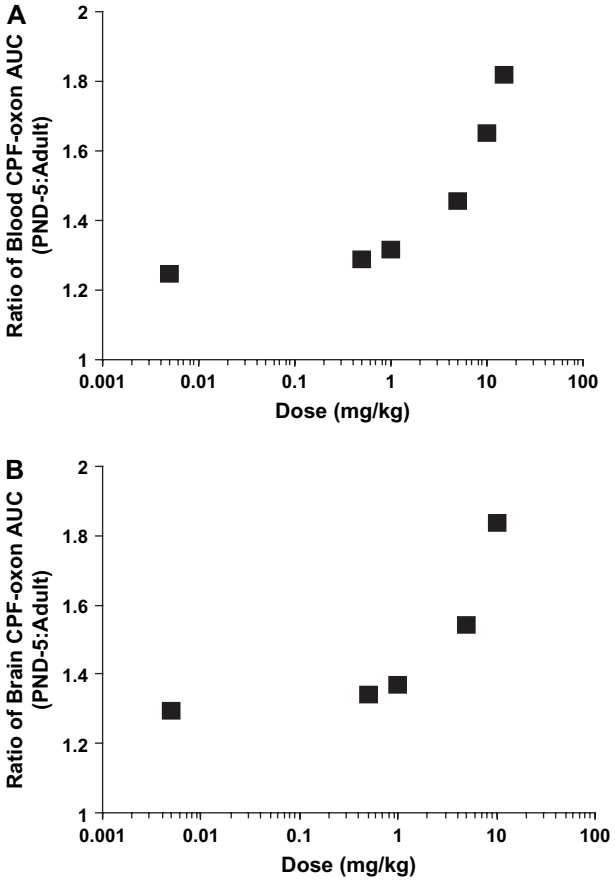

FIG. 13. The ratio of (A) blood and (B) brain CPF-oxon $AUC_{0-\alpha}$ comparing neonatal (PND-5) and adult rats PND-5(AUC)/Adult(AUC) following simulation of an acute oral exposure to a broad range of CPF doses.

bimolecular inhibitory rate constant (K_i) for brain AChE binding/inhibition will also be an important determinant of brain AChE inhibition. For all analyses, the metabolic parameters (K_m and Vmax) associated with CYP450 and PON-1 metabolism were more sensitive in PND-5 versus adult rats with regard to brain AChE inhibition. The model was more sensitive to changes in hepatic PON-1 than to blood activity, which would be consistent with the importance of the liver for overall metabolism (activation as well as detoxification). As expected, the model was very sensitive to changes in the K_i for brain AChE inhibition, especially in PND-5 animals relative to the adults. The greater sensitivity in the PND-5 rats may be associated with an approximate 4× higher K_i for CPF-oxon binding to AChE than is seen in the adult rat. Since these parameters were measured *in vitro* (Kousba *et al.*, 2007), there is confidence in utilizing these different age-dependent parameter estimates. Overall, the PND-5 preweanling rats appeared to be more sensitive to slight changes in model parameters than the adult rats, and they were particularly sensitive to changes in CYP450-related metabolism (activation and detoxification).

TABLE 6
Selected PBPK/PD Model Maximum Sensitivity Coefficient Ranking for PND-5 and Adult Rats following a Single Oral Gavage Exposure to 5 mg CPF/kg of Body Weight

	PND-5		Adult	
Parameters	Sensitivity ranking[a]	Uncertainty designation[b]	Sensitivity ranking[a]	Uncertainty designation[b]
CYP				
CPF to TCP Vmax	H	M	VL	L
CPF to TCP K_m	H	M	VL	L
CPF to CPF-oxon Vmax	H	M	VL	L
CPF to CPF-oxon K_m	H	M	VL	L
PON1 (CPF-oxon to TCP)				
Hepatic Vmax	M	M	VL	L
Hepatic K_m	M	M	VL	L
Blood Vmax	VL	M	VL	L
Blood K_m	VL	M	VL	L
Blood flow				
Hepatic	H	H	VL	L
Brain	M	H	VL	L
Tissue volume				
Hepatic	VL	M	VL	L
Brain	VL	M	VL	L
Fat	VL	M	VL	L
Brain AChE				
Bimolecular inhibition (K_i)	H	L	VL	L
Basal enzyme activity	M	M	VL	M

Note. For this analysis brain ChE was utilized as the relevant model response to evaluate the impact of changes in specified model parameters.

[a]**Sensitivity ranking:** Very low (VL): sensitivity coefficient (SC) < 0.1; low (L): SC range 0.1–0.25. Medium (M): SC range 0.25–0.5; high (H): SC range ≥ 0.5. The determination of sensitivity is time-dependent; hence the sensitivity ranking was determined from the greatest value regardless of time achieved. Parameters for SC < 0.1 were not reported or considered further in this analysis.

[b]**Uncertainty designation:** Sensitivity parameters were qualitatively categorized low, medium, or high uncertainty. Low (L): experimentally determined in rat; medium (M): scaled value from a different species or optimized based on multiple data sets; high (H): parameters optimized from limited data or lacking published or historical values.

DISCUSSION

Previous studies suggest that juvenile rats are sensitive to the high-dose toxicity of OP insecticides, and a lack of maturation in detoxification pathways appears to be a contributing factor (Atterberry *et al.*, 1997; Li *et al.*, 1997; Mortensen *et al.*, 1996, 1998). It has been proposed that PBPK/PD models can be applied to assess this age-dependent sensitivity (Clewell *et al.*, 2004; Ginsberg *et al.*, 2004; Price *et al.*, 2003; Timchalk, 2001). The current paper extends our previously developed rodent PBPK/PD model for CPF by incorporating age-dependent physiological and metabolic parameters.

In this model, age was utilized as a dependent function to estimate body weight, and organ growth was determined as a percentage of body weight. Liver and brain volumes were

based on best-fit polynomial equations (see Fig. 2 and supplemental data). This approach was comparable to the scaling approach applied to characterize physiological and anatomical changes from birth to adolescence in humans (Haddad *et al.*, 2001). However, due to limited amounts of juvenile rat data it was not feasible to develop comprehensive age-dependent scaling algorithms as has been done for human models (Clewell *et al.*, 2004; Price *et al.*, 2003). The default approach for cross species scaling of metabolism is to scale the metabolic rate as the 3/4th power of body weight ($Vmax = VmaxC \times Bwt^{0.74}$) (Krishnan and Andersen, 1994). In the current model, alternative scaling exponents were developed (see Tables 2 and 4) for CYP450 and PON-1 metabolism and for B-est tissue levels based upon published data in the preweanling rat (Atterberry *et al.*, 1997; Carr *et al.*, 2000; Mortensen *et al.*, 1996, 1998; Tang *et al.*, 1999).

Knaak *et al.* (2004) reviewed the physiochemical and biological literature needed to develop OP insecticide PBPK/PD models, and noted that many of the *in vitro* and *in vivo* data needed for model development are inadequate or lacking. To this end, *in vivo* and *in vitro* pharmacokinetic/PD studies were previously conducted to provide needed experimental data to facilitate model development (Kousba *et al.*, 2007; Timchalk *et al.*, 2006). Based on the observed blood time-course of CPF, absorption following gavage oral administration in the preweanling rat was relatively rapid (see Figure 5; C_{max} 3–6 h) and consistent with the absorption rate previously seen in the adult rat (see Figure 4A). Hence, the current model utilized the same structure and parameter estimates to determine the absorption rate as previously described (Timchalk *et al.*, 2002). It was assumed that absorption from the gut was complete at all ages; this simplifying assumption was done in full recognition that the extent of oral absorption has been shown to be variable and dependent upon the dose formulation (Nolan *et al.*, 1984; Timchalk *et al.*, 2002). However, there are supporting data suggesting that absorption for a number of xenobiotics in both rodents and humans may be greater in juveniles than for adults (Ginsberg *et al.*, 2004).

Of particular importance was the observation that even in rats as young as PND-5, the CYP450 metabolic capacity was adequate to metabolize CPF to both TCP and CPF-oxon based on the detection of TCP in blood and extensive ChE inhibition. In addition, the increase in the blood TCP concentration (~3-fold) in PND-17 rats relative to the response in the younger animals, and the lower blood concentrations of CPF (1.7 to 7.5-fold) in adults (Timchalk *et al.*, 2002) relative to preweanling rats is consistent with an increase in CYP450 metabolic capacity with age. This suggests that CPF was rapidly absorbed and metabolized, and the extent of metabolism was age-dependent.

The current model is capable of predicting B-est inhibition based upon the stoichiometric enzyme interaction with CPF-oxon. The extent and rate of B-est inhibition and recovery is dependent upon the amount of available enzyme, the bimolecular inhibition rate constant (K_i), and the exposure duration (Vale, 1998). The relative quantity of available B-est binding sites (μmol) followed the general order: CaE $\gg$ BuChE > AChE as was previously described for the adult rat (Maxwell *et al.*, 1987; Timchalk *et al.*, 2002). Age-related changes in regional brain distribution of AChE and the molecular forms of the enzyme have been reported (Bisso *et al.*, 1991; Mendeguz *et al.*, 1992; Skau and Triplett, 1998). Although age-dependent changes in K_i values have not been extensively investigated, our research group has recently reported age-dependent differences in the apparent K_i values for CPF-oxon (Kousba *et al.*, 2007). Studies suggest that K_i differences could be related to the presence of a secondary peripheral binding site, which can impact the capability of the substrate to reach the active site of AChE (Kousba *et al.*, 2004; Taylor and Radic, 1994). The potential for CPF-oxon to interact with secondary proteins that modify the binding affinity of the oxon with AChE is also feasible; in this regard, Murphy (1982) suggested that a lower toxicity in adult rats may be in part due to a higher binding of the oxon to noncritical tissues in the brain. Consistent with this hypothesis, Mortensen *et al.* (1998) showed that the brain protein concentrations increased from 7% to ~12% from PND-4 to -90. Regardless of the specific underlying mechanism for the observed age-related differences in the apparent K_i parameters, the use of the measured K_i parameters (Kousba *et al.*, 2007) for tissue AChE enables the model to reasonably simulate tissue ChE as a function of age and dose in the rat.

In the current study the model-predicted ChE inhibition is generally comparable with the experimentally determined results which are also consistent with the observed age-dependent sensitivity of juvenile rats (Atterberry *et al.*, 1997; Benke and Murphy, 1975; Broderu and DuBois, 1963; Gaines and Linder, 1986; Harbison, 1975; Mortensen *et al.*, 1996, 1998; Moser and Padilla, 1998). Of importance is the magnitude of the age- and dose-dependent inhibition of brain AChE. In the preweanling rats, the dose–response for brain AChE was very steep as demonstrated by the limited inhibition predicted by the model at 1 mg/kg (78–98% of control), but substantial inhibition (16–41% of control) at 10 mg/kg (see Figs. 9A–C). In adult rats we have previously noted (Timchalk *et al.*, 2002) a similar steep dose–response for brain AChE inhibition which occurs at doses > 10 mg/kg; whereas, in the current study doses that produce substantial brain AChE inhibition in preweanling rats (10 mg/kg) resulted in minimal to no AChE inhibition (85–103% of control; Fig. 9D) in adults. This observation is consistent with the model simulations comparing the ratio of blood and brain CPF-oxon AUC of PND-5 and adult rats (see Fig. 13) that suggest a disproportionate increase in oxon levels in preweanlings relative to adults. This increase in blood and brain CPF-oxon concentration is consistent with the hypothesis that the greater sensitivity of preweanling rats is primarily due to a lack of maturation in detoxification pathways, as has been suggested by a number of other investigators (Atterberry *et al.*, 1997; Li *et al.*, 1997; Mortensen *et al.*, 1996, 1998).

Although the PBPK/PD model simulates the overall age-dependent dosimetry and ChE inhibition response, not all of the experimental data are as well described by the model, which suggests some potential areas for improvement in model structure (i.e., inadequate description of the biological system) or inadequate model parameterization, and future research needs. For example, in the preweanling rats (see Fig. 5) the simulations of CPF blood concentrations generally underpredicted the experimental data and suggested a faster blood clearance than was experimentally determined. These observed dosimetry differences suggest that rates of absorption, changes in tissue distribution and protein binding characteristics, or the extent of CYP450 metabolism may not be adequately characterized. Likewise, with regard to plasma ChE, the model consistently overpredicted peak preweanling inhibition (Table 5, A; Figs. 7 and 12), even when we increased the reported plasma AChE activity by a factor of 10, yet more reasonably simulated the RBC AChE response (Table 5, B, Figs. 8 and 12). This observed difference may be related to the complexity of the plasma where three B-est enzymes (AChE, BuChE and CaE) are present and function to stoichiometrically bind with and detoxify CPF-oxon. Of the three B-est, AChE was the only enzyme where age-dependent data for the bimolecular inhibition rate constant (K_i) were determined (Kousba *et al.*, 2007) in brain and applied to all tissue (plasma, RBC, diaphragm, and liver); whereas, in the current model the inhibition rate constants for BuChE and CaE were maintained at the adult levels. The complexity of the plasma compartment with regard to B-est activity could contribute to the observed difference in plasma ChE response relative to RBC AChE. Further refinement of the model fit may be possible by obtaining additional experimental data to define these potential age-dependent model parameters. Finally, one of the important functional limitations of the current model is that it does not take into account observed cholinergic toxicity which is clearly known to modify a range of physiological and metabolic parameters (see Lotti, 2001). Hence, some of the poorer fits to experimental data particularly at acutely toxic doses may be partially accounted for by this limitation in the current model structure.

The PBPK/PD model developed here represents one potential computational framework for development of an age-dependent human model. As noted by Ginsberg *et al.* (2004), current risk assessment methods utilize an across species extrapolation that is typically done between adults; however, based on similar patterns for developmental ontogeny of metabolism and clearance mechanisms the evaluation of toxicity in juvenile animals may have more direct relevance to children. Therefore, the development of age-dependent models offers great promise to better identify ''early life-stage'' related sensitivity (Clewell *et al.*, 2004; Price *et al.*, 2003). In general, metabolic functions develop over the first 2–3 weeks in rats and 2–3 months in children (Ginsberg *et al.*, 2004). However, there is still considerable uncertainty concerning the species-specific developmental rates of pharmacokinetic systems, particularly in juvenile animals where there are limited data. There is a need to continue developing new data with animal models that can then be used to facilitate the extrapolation and development of early life-stage models in humans. Nonetheless, early life-stage models are being developed and applied to children (Clewell *et al.*, 2004; Pelekis *et al.*, 2001; Price *et al.*, 2003). The development of comparable life-stage animal models holds great promise to enhance age- and species-specific dosimetry and dynamic response extrapolations and should reduce the uncertainty associated with age-specific risk assessments.

In summary, these results indicate that the age-dependent PBPK/PD model behaves consistently with the general understanding of CPF toxicity, pharmacokinetics, and tissue ChE inhibition in neonatal and adult rats. Secondly, the model suggests that neonatal rats are quantitatively more sensitive to the high-dose acute effects of CPF exposure than adult rats. Future research must entail further development and validation with the ultimate goal of developing a model that is capable of predicting biological response in infants and children.

SUPPLEMENTARY DATA

Supplementary data are available online at http://toxsci.oxfordjournals.org/.

FUNDING

Centers for Disease Control and Prevention (R01 OH003629-04, R01 OH008173-01); U.S. EPA's STAR program (R828608).

ACKNOWLEDGMENTS

The contents of this paper are solely the responsibility of the authors and have not been subject to any review by CDC or EPA and therefore do not necessarily represent the official view of CDC or EPA, and no official endorsement should be inferred.

REFERENCES

Alcorn, J., and McNamara, P. J. (2002). Ontogeny of hepatic and renal systemic clearance pathways in infants. Part II. *Clin. Pharmacokinet.* **41,** 1077–1094.

Atterberry, T. T., Burnett, W. T., and Chambers, J. E. (1997). Age-related differences in parathion and chlorpyrifos toxicity in male rats: Target and nontarget esterase sensitivity and cytochrome P450-mediated metabolism. *Toxicol. Appl. Pharmacol.* **147,** 411–418.

Augustinsson, K-B., and Barr, M. (1963). Age variation in plasma arylesterase activity in children. *Clin. Chem. Acta* **8,** 568–573.

Benke, G. M., and Murphy, S. D. (1975). The influence of age on the toxicity and metabolism of methyl parathion and parathion in male and female rats. *Toxicol. Appl. Pharmacol.* **31,** 254–269.

Bisso, G. M., Briancesco, R., and Michalek, H. (1991). Size and charge isomers of acetylcholinesterase in the cerebral cortex of young and aged rats. *Neurochem. Res.* **16**(5), 571–575.

Brodeur, J., and DuBois, K. P. (1963). Comparison of acute toxicity of anticholinesterase insecticides to weanling and adult male rats. *Proc. Soc. Exp. Biol. Med.* **114,** 509–511.

Byczkowski, J. Z., Kinkead, E. R., Leahy, H. F., Randall, G. M., and Fisher, J. W. (1994). Computer simulation of the lactational transfer of tetrachloroethylene in rats using a physiologically based model. *Toxicol. Appl. Pharmacol.* **125,** 228–236.

Carr, R. L., Chambers, H. W., Guarisco, J. A., Richardson, J. R., Tang. J., and Chambers, J. E. (2001). Effects of repeated oral postnatal exposure to chlorpyrifos on open-field behavior in juvenile rats. *Toxicol. Sci.* **59,** 260–267.

Chambers, J. E., and Chambers, H. W. (1989). Oxidative desulfation of chlorpyrifos, chlorpyrifos-methyl, and leptophos by rat brain and liver. *J. Biochem. Toxicol.* **4**(1), 201–203.

Chanda, S. M., Mortensen, S. R., Moser, V. C. And Padilla, S. (1997). Tissue-specific effects of chlorpyrifos on carboxylesterase and cholinesterase activity in adult rats: An *in vitro* and *in vivo* comparison. *Fundam. Appl. Toxicol.* **38,** 148–157.

Clewell, H. J., Gentry, P. R., Covington, T. R., Sarangapani, R., and Teeguarden, J. G. (2004). Evaluation of the potential impact of age- and gender-specific pharmacokinetic differences on tissue dosimetry. *Toxicol. Sci.* **79,** 381–393.

Clewell, H. J., Teeguarden, J., McDonald, T., Sarangapani, R., Lawrence, G., Covington, T., Gentry, R., and Shipp, A. (2002). Review and evaluation of the potential impact of age- and gender-specific pharmacokinetic differences on tissue dosimetry. *Crit. Rev. Toxicol.* **32,** 329–389.

Clewell, R. A., Merrill, E. A., Yu, K. O., Mahle, D. A., Sterner, T. R., Fisher, J. W., and Gearhart, J. M. (2003). Predicting neonatal perchlorate dose and inhibition of iodide uptake in the rat during lactation using physiologically-based pharmacokinetic modeling. *Toxicol. Sci.* **74**(2), 416–436.

Corley, R. A., Mast, T. J., Carney, E. W., Rogers, J. M., and Daston, G. P. (2003). Evaluation of physiologically based models of pregnancy and lactation for their application in children's health risk assessment. *Crit. Rev. Toxicol.* **33**(2), 137–211.

Domoradzki, J. Y., Marty, M. S., Hansen. S. C., Timchalk, C., and Mattsson, J. L. (2004). Effect of different dosing paradigms on the body burden of chlorpyrifos in neonatal Sprague-Dawley rats. *Toxicol. Sci.* **78**(1-S), 104 (Abstract).

Fisher, J.W., Whittaker, T.A., Taylor, D.H., Clewell, H. J. III, and Andersen, M. E. (1990). Physiologically based pharmacokinetic modeling of the lactating rat and nursing pup: A multiroute model for trichloroethylene and its metabolite, trichloroacetic acid. *Toxicol. Appl. Pharmacol.* **102,** 497–513.

FQPA. (1996). Food Quality Protection Act, Public Law No. 104–170.

Gaines, T. B., and Linder, R. E. (1986). Acute toxicity of pesticides in adult and weanling rats. *Fundam. Appl. Toxicol.* **7,** 172–178.

Gearhart, J. M., Jepson, G. W., Clewell, H. J. III, Andersen, M. E. and Connolly, R. B. (1990). Physiologically based pharmacokinetic and pharmacodynamic model for the inhibition of acetylcholinesterase by diisopropylfluorophosphate. *Toxicol. Appl. Pharmacol.* **106,** 295–310.

Gentry, P. R., Habaer, L. T., McDonald, T. B., Zhao, Q., Covington, T., Nance, P., Clewell III, H. J., Lipscomb, J. C., and Barton, H. A. (2004). Data for physiologically based pharmacokinetic modeling in neonatal animals: Physiological parameters in mice and Sprague-Dawley rats. *J. Child. Health* **2**(3–4), 363–411.

Ginsberg, G., Hattis, D., and Sonawane, B. (2004). Incorporating pharmacokinetic differences between children and adults in assessing children's risk to environmental toxicants. Parameters in mice and Sprague-Dawley rats. *Toxicol. Appl. Pharmacol.* **198,** 164–183.

Haddad, S., Restieri, C., and Krishnan, K. (2001). Characterization of age-related changes in body weight and organ weights from birth to adolescence in humans. *J. Toxicol. Environ. Health Part A* **64,** 453–464.

Harbison, R. D. (1975) Comparative toxicity of some selected pesticides in neonatal and adult rats. *Toxicol. Appl. Pharmacol.* **32,** 443–446.

Johnson, T. N. (2003). The development of drug metabolizing enzymes and their influence on the susceptibility to adverse drug reactions in children. *Toxicology* **192,** 37–48.

Knaak, J. B., Dary, C. C., Power, F., Thompson, C. B., and Blancato, J. N. (2004). Physicochemical and biological data for the development of predictive organophosphorus pesticide QSARs and PBPK/PD models for human risk assessment. *Crit. Rev. Toxicol.* **34**(2), 143–207.

Kousba, A. A., Poet, T. S., and Timchalk, C. (2007). Age-related brain cholinesterase inhibition kinetics following *in vitro* incubation with chlorpyrifos-oxon and diazinon-oxon. *Toxicol. Sci.* **95**(1), 147–155.

Koubsa, A. A., Sultatos, L. G., Poet, T. S., and Timchalk, C. (2004). Comparison of chlorpyrifos-oxon and paraoxon acetylcholinesterase inhibition dynamics: Potential role of a peripheral binding site. *Toxicol. Sci.* **80,** 239–248.

Krishnan, K., and Andersen, M. E. (1994). Physiologically based pharmacokinetic modeling in toxicology. *Principles and Methods of Toxicology*, 3rd ed. (A.W. Hayes, Ed.), pp. 149–188, Raven Press, New York.

Li, W. F., Matthews, C., Disteche, C. M., Costa. L. G., and Furlong, C. E. (1997). Paraoxonase (PON1) gene in mice: Sequencing, chromosomal localization and developmental expression. *Pharmacogenetics* **7,** 137–144.

Lotti, M. (2001). Clinical toxicology of anticholinesterase agents in humans. In *Handbook of Pesticide Toxicology* (R. I. Krieger, Ed.), pp. 1043–1085. Academic Press, San Diego, CA.

Lowe, E. R., Rick, D. L., West, R. J., and Bartels, M. J. (2006). The evaluation of quantitative structure property relationship predictions of tissue-blood partition coefficients of highly lipophilic chemicals. *Drug Metab. Rev.* **38,** 78.

Ma, T., and Chambers, J. E. (1994). Kinetic parameters of desulfuration and dearylation of parathion and chlorpyrifos by rat liver microsomes. *Food Chem. Toxicol.* **32**(8), 763–767.

Makri, A., Goveia, M., Balbus, J., and Parkin, R. (2004). Children's susceptibility to chemicals: A review by development stage. *J. Toxicol. Environ. Health Part B* **7,** 417–435.

Maxwell, D. M., Lenz, D. E., Groff, W. A., Kaminskis, A., and Froehlich, H. L. (1987). The effect of blood flow and detoxification on *in vivo* cholinesterase inhibition by soman in rats. *Toxicol. Appl. Pharmacol.* **88,** 66–76.

Mendeguz, A., Bisso, G. M., and Michalek, H. (1992). Age-related changes in acetylcholinesterase and its molecular forms in various brain areas of rats. *Neurochem. Res.* **17**(8), 785–790.

Miller, M. S., McCarver, D. G., Bell, D. A., Eaton, D. L., and Goldstein, J. A. (1997). Genetic polymorphisms in human drug metabolic enzymes. *Fundam. Appl. Toxicol.* **40,** 1–14.

Mortensen, S. R., Chanda, S. M., Hooper, M. J., and Padilla, S. (1996). Maturational differences in chlorpyrifos-oxonase activity may contribute to age-related sensitivity to chlorpyrifos. *J. Biochem. Toxicol.* **11**(6), 279–287.

Mortensen, S. R., Hooper, M. J., and Padilla, S. (1998). Rat brain acetylcholinesterase activity: Developmental profile and maturational sensitivity to carbamate and organophosphorus inhibitors. *Toxicolology* **125**, 13–19.

Moser, V. C., and Padilla, S. (1998). Age- and gender-related differences in the time-course of behavioral and biochemical effects produced by oral chlorpyrifos in rats. *Toxicol. Appl. Pharmacol.* **149,** 107–119.

Mueller, R. F., Hornung, S., Furlong, C. E., Anderson, J., Giblett, E. R., and Motulsky, A. G. (1983). Plasma paraoxonase polymorphism: A new enzyme assay, population, family, biochemical and linkage studies. *Am. J. Hum. Genet.* **35,** 393–408.

Murphy, S. D. (1982). Toxicity and hepatic metabolism of organophosphate insecticides in developing rat. In *Environmental Factors in Human Growth and Development* (V. R. Hunt, M. K. Smith, and D. Worth, Eds.), Report No. 11, pp. 125–134. Gold Spring Harbor Laboratory, New York.

Murphy, S. D. (1986). Toxic effects of pesticides. In *Casarett and Doull's Toxicology, The Basic Science of Poison*, 3rd ed. (C. D. Klaassen, M. O. Amdur, and J. Doull, Eds.), pp. 519–581. MacMillam Publishers, New York.

National Academy of Sciences. (1993). Pesticides in the diets of children. *Natl. Acad. Sci.* Washington, DC.

Nolan, R. J., Rick, D. L., Freshour, N. L., and Saunders, J. H. (1984). Chlorpyrifos: Pharmacokinetics in human volunteers. *Toxicol. Appl. Pharmacol.* **73,** 8–15.

Pelekis, M., Gephart, L. A., and Lerman, S. E. (2001). Physiological-model-based derivation of the adult and child pharmacokinetic intraspecies uncertainty factors for volatile organic compounds. *Regul. Toxicol. Pharmacol.* **33,** 12–20.

Poet, T. S., Wu, H., Kousba, A. A., and Timchalk, C. (2003). In vitro rat hepatic and enterocyte metabolism of the organophosphate pesticide chlorpyrifos and diazinon. *Toxicol. Sci.* **72,** 193–200.

Pope, C. N., Chakraborti, T. K., Chapman, M. L., Farrar, J. D., and Arthun, D. (1991). Comparison of the *in vivo* cholinesterase inhibition in neonatal and adult rats by three organophosphorothioate insecticides. *Toxicology* **68,** 51–61.

Pope, C. N., and Liu, J. (1997). Age-related differences in sensitivity to organophosphosphorus pesticides. *Environ. Toxicol. Pharmacol.* **4,** 309–314.

Price, K., Haddad, S., and Krishnan, K. (2003). Physiological modeling of age-specific changes in the pharmacokinetics of organic chemicals in children. *J. Toxicol. Environ. Health Part A* **66,** 417–433.

Schoeffner, D. J., Warren, D. A., Muralidhara, S., Bruckner, J. V. and Simmons, J. E. (1999). Organ weights and fat volume in rats as a function of strain and age. *J. Toxicol. Environ. Health Part A* **56,** 449–462.

Skau, K.A., and Triplett, C. G. (1998). Age-related changes in activity of Fischer 344 rat brain acetylcholinesterase molecular forms. *Mol. Chem. Neuropathol.* **35**(1–3), 13–21.

Sultatos, L. G. (1994). Mammalian toxicology of organophosphorus pesticides. *J. Toxicol. Environ. Health* **43,** 271–289.

Sundberg, J., Jonsson, S., Karlsson, M. O., Hallen, I., and Oskarson, A. (1998). Kinetics of methylmercury and inorganic mercury in lactating and non-lactating mice. *Toxicol. Appl. Pharmacol.* **151,** 319–329.

Tang, J., Cao, Y., Rose, R. L., Brimfield, A. A., Dai, D., Goldstein, J. A., and Hodgson, E. (2001). Metabolism of chlorpyrifos by human cytochrome PCYP isoforms and human, mouse and rat liver microsomes. *Drug Metab. Dispos.* **29,** 1201–1204.

Tang, J., Carr, R. L., and Chambers, J. E. (1999). Changes in rat brain cholinesterase activity and muscarinic receptor density during and after repeated oral exposure to chlorpyrifos in early postnatal development. *Toxicol. Sci.* **51,** 265–272.

Taylor, P., and Radic, Z. (1994). The cholinesterases: From genes to proteins. *Annu. Rev. Pharmacol. Toxicol.* **34,** 281–320.

Teeguarden, J. G., Deisinger, P. J., Poet, T. S., English, J. C., Faber, W. D., Barton, H. A., Corley, R. A., and Clewell, H. J., III (2005). Derivation of a human equivalent concentration for n-butanol using a physiologically-based pharmacokinetic model for n-butyl acetate and metabolites n-butanol and n-butyric acid. *Toxicol. Sci.* **85,** 429–446.

Timchalk, C. (2001). Organophosphate pharmacokinetics, chapter 46. In *Hayes' Handbook of Pesticide Toxicology*, 2nd ed. (R. J. Krieger Ed.), pp. 929–951. Academic Press, San Diego, CA.

Timchalk, C., Nolan, R. J., Mendrala, A, L., Dittenber, D. A., Brzak, K. A., and Mattsson, J. L. (2002). A physiologically based pharmacokinetic and pharmacodynamic (PBPK/PD) model for the organophosphate insecticide chlorpyrifos in rats and humans. *Toxicol. Sci.* **66**(1), 34–53.

Timchalk, C., Poet, T. S. and Kousba, A. A. (2006). Age-dependent pharmacokinetic and pharmacodynamic response in preweanling rats following oral exposure to the organophosphorus insecticide chlorpyrifos. *Toxicology* **220,** 13–25.

Vale, J. A. (1998). Toxicokinetic and toxicodynamic aspects of organophophate (OP) insecticide poisoning. *Toxicol. Lett.* **102–103,** 649–652.

Won, Y. K., Liu, J., Olivier, K., Jr, Zheng, Q., and Pope, C. N. (2001). Age-related effects of chlorpyrifos on acetylcholine release in rat brain. *NeuroToxicology* **22,** 39–48.

Zheng, Q., Olivier, K., Won, Y. K., and Pope, C. N. (2000). Comparative cholinergic neurotoxicity of oral chlorpyrifos exposures in preweanling and adult rats. *Toxicol. Sci.* **55,** 124–132.